Return to P6Elle

12

Los Alamos Environmental Restoration Records Processing Facility

INC-DO
MS J519

ER Record I.D.# 0008887

Final Report

on

A Pilot Study on the Applicability of Selected Geophysical Methods to the Investigation of Three Environmental Sites in TA-49, Los Alamos National Laboratory

(Contract Number: 9-L61-W0086-1)

Submitted to

Los Alamos National Laboratory
Los Alamos, NM 87545

by

Geophex, Ltd.
605 Mercury Street
Raleigh, NC 27603-2343
(919)839-8515
Fax (919)839-8528

Geophex Job No. 229

August 1, 1991

Geophex, Ltd.
terram et marum exploramus

14306

Geophex, Ltd
605 Mercury Street
Raleigh, North Carolina 27603
(919) 839-8515

August 1, 1991

Dr. P. Gary Eller; (505)667-0835
P.O. Box 1663, MS J519
Los Alamos National Laboratory
Los Alamos, New Mexico 87545

Subject: Final Report on Geophysical Studies at TA-49, 3 Sites, LANL;
Contract 9-L61-W0086-1

Dear Dr. Eller:

Enclosed are two copies of Final Report on the subject contract. Should you have any comments or suggestions on revision, please let me know. We enjoyed working with you and your staff on this project and hope to continue providing our service to LANL.

Sincerely,

I.J. Won, PhD, PG
Technical Director

cc: Dr. Jim Aldrich (with report)
MS D462, LANL

IJW/ah

Table of Contents

Page

1.0 Scope of Work 1

2.0 Tested Geophysical Methods and Instruments 2
2.1 Magnetic Method 4
2.2 Electromagnetic Method 5
2.3 Ground-Penetrating Radar 7

3.0 Results 9
3.1 Area 4 (Test Shafts) 10
3.2 Area 11 (Leach Field) 10
3.3 Landfill/Trash-Burning Area 12

4.0 Conclusions and Recommendations 13

References 14

Figures . . . . . 15 thru 41

Appendix A. Technical Description of GEM-1

List of Figures:

Figure 1.0-1. Areal map of TA-49, Los Alamos National Laboratory.
Figure 1.0-2. Site map of Area 4 (Test Shafts).
Figure 1.0-3. Site map of Area 11 (Leach Field).
Figure 1.0-4. Site map of Landfill.

Figure 2.1-1. Photograph of magnetic survey and two example contoured magnetic maps over an underground storage tank. The sensor height is 2 feet (left) and 5 feet (right).
Figure 2.2-1. Photograph of electromagnetic survey; an example EM anomaly over a UST (parallelogram). Also shown to the right is a nomogram showing the relationship between source frequency, ground conductivity, and depth of penetration (skin depth).
Figure 2.3-1. Photograph of GPR survey and two GPR records over a UST.

Figure 3.1-1. Area 4 (Test Shafts): total field magnetic map (in gamma); Background = 51,600 gamma; Contour interval = 400 gamma.
Figure 3.1-2. Area 4: Magnetic gradient map (in gamma/m); Contour interval = 400 gamma/m. The fish-net view is shown upside down for a clear view.
Figure 3.1-3. Area 4: Electromagnetic data (in ppm); 800 Hz; Contour interval = 400 ppm.
Figure 3.1-4. Area 4: Fish-net view of electromagnetic data (in ppm); 800 Hz Inphase.

Figure 3.1-5. Area 4: Electromagnetic data (in ppm); 3,200 Hz; Contour interval = 400 ppm.
Figure 3.1-6. Area 4: Electromagnetic data (in ppm); 9,600 Hz; Contour interval = 400 ppm.
Figure 3.1-7. Area 4: A typical GPR profile near the suspect shafts area.
Figure 3.1-8. Area 4 (Test Shafts): Interpretive sketch based on geophysical data and field observation.

Figure 3.2-1. Area 11 (Leach Field): total field magnetic map (in gamma); Background = 52,000 gamma; Contour interval = 200 gamma.
~~Figure 3.2-2. Area 11: Magnetic gradient map (in gamma/m); Contour interval = 200 gamma/m.~~ The fish-net view is shown upside down for a clear view.
Figure 3.2-3. Area 11: Electromagnetic data (in ppm); 800 Hz; Contour interval = 200 ppm.
Figure 3.2-4. Area 11: Electromagnetic data (in ppm); 3,200 Hz; Contour interval = 200 ppm.
Figure 3.2-5. Area 11: Electromagnetic data (in ppm); 9,600 Hz; Contour interval = 200 ppm.
Figure 3.2-6. Area 11 (Leach Field): Interpretive sketch based on geophysical data and field observation.

Figure 3.3-1. Landfill: Total field magnetic map (in gamma); Background = 52,200 gamma; Contour interval = 400 gamma.
Figure 3.3-2. Landfill: Electromagnetic data (in ppm); 800 Hz; Contour interval = 400 ppm.
Figure 3.3-3. Landfill: Fish-net view of electromagnetic data (in ppm); 800 Hz Inphase data.
Figure 3.3-4. Landfill: Electromagnetic data (in ppm); 3,200 Hz; Contour interval = 400 ppm.
Figure 3.3-5. Landfill: Electromagnetic data (in ppm); 9,600 Hz; Contour interval = 400 ppm.
Figure 3.3-6. Landfill: Interpretive sketch based on geophysical data and field observation.

1.0 Scope of Work

On May 21, 1991, Los Alamos National Laboratory (LANL) issued Geophex a contract entitled "Geophysical Survey at Three Solid Waste Management Units (SWMUs)." These SWMUs, located within a fenced compound of TA-49, LANL, are shown in Figure 1.0-1. A brief description of each site, as provided by LANL, follows:

- Area 4 (Figure 1.0-2) was a materials disposal area containing buried metal test-shafts, pipes, and other structures as well as disturbed soils. The area has dimensions approximately 125 by 125 feet, contains radioactive wastes, and is suspected of containing hazardous wastes. The objectives of the geophysical survey are to locate metal structures, disturbed soils, and to verify existing drawings.

- Area 11 (also known as SWMU #49-003; Figure 1.0-3) was a radiochemical leach field. The leach field has dimensions approximately 65 by 40 feet and contains both radioactive and hazardous wastes. The objectives of the geophysical survey are to locate the boundaries of the leach field and associated metal structures.

- The exact location and dimensions of the Landfill site (also known as SWMU #49-004; Figure 1.0-4) are unknown. The site is designated as "Trash Burning Area" in Figure 1.0-1. No radioactive or hazardous wastes are known to be present at the site. The objective of the geophysical survey is to define the boundaries of the trenches at the site.

Geophex was advised by the LANL Project Manager that the intent of this study was to investigate the applicability of various geophysical methods to the preliminary environmental assessment of some typical LANL SWMU sites. Most of these SWMUs are within a geological unit known as the Bandelier Tuff. The investigation was not to be considered a full-scale site characterization, but rather a pilot geophysical study for delineating buried targets within this geological environment.

After reviewing available technical data, a previous similar study by LANL, and area geology, as well as having considerable discussions with several LANL scientists and managers, Geophex proposed (and LANL accepted) the trials of the following three geophysical methods and instruments at the subject TA-49 SWMUs:

- Total field magnetic survey;: EG&G Geometrics G-846 Proton Precession Magnetometer;
- Electromagnetic survey: Geophex GEM-1 Multi-frequency Digital Electromagnetic Unit; and
- Ground-penetrating radar (GPR): GSSI SIR System-3.

Geophysical field survey was conducted by a three-man crew from Geophex from June 5 through June 10. In all occasions, the survey crew was escorted by the LANL staff into TA-49. At Sites 4 and 11, additionally fenced areas within TA-49 where radioactive wastes are assumed to be buried, the survey crew wore coveralls (LANL ANTI-C), protective boots, and plastic gloves; and went

through radiation checks by the LANL health staff at the end of each survey period.

Some rudimentary data plots were made concurrently with the survey. On the morning of June 11, we held an exit briefing for about a dozen LANL technical staff and presented and discussed our initial findings based on the preliminary data.

2.0 Tested Geophysical Methods and Instruments

Since this project is conceived as a pilot project for determining the applicabilities of certain geophysical methods to the LANL SWMUs, we start with a brief, heuristic discussion on the overall geophysical methods and their abilities to detect certain target objects buried in a given geologic medium.

The major advantages of geophysical methods in an environmental investigation may include:

- Minimal Intrusion: thus, inherently safe for the initial phases of a site characterization process for SWMUs where hazardous materials are suspected;

- Synoptic Description of the Site: owing to rapid coverage over a large area, the method can pinpoint, by eliminating portions of the site, locations for further studies such as boring and sampling; the method can be used for both reconnaissance and delineation phases;

- Large Search Radius: because most geophysical sensors have finite "foot prints" or search swaths, they have less chance of "missing" the target by a short distance, which is common to boring and drilling; and

- Cost Effectiveness: owing to the above attributes, the methods can provide relatively high returns on the volume of information versus cost incurred.

All geophysical methods look for the contrasts in certain basic physical properties between the target and the host medium. Despite their diversities, all geophysical tools are based on a few simple physical laws derived mostly from the classical physics of gravity, electricity, magnetism, and mechanics. Broadly speaking, they are grouped into two categories: active and passive sensors. An active sensor emits a source field and measures response of the target; this includes seismic, electromagnetic, GPR, and some types of electrical and radioactive surveys. A passive sensor measures some ambient field that is warped by a hidden target; this includes gravity, magnetics, natural radioactivity, and some types of electrical surveys.

Seismic and GPR sensors emit short acoustic or electromagnetic pulses and measure the echoes or other responses from objects hidden in the earth. For the seismic method, the amplitude and phase of the returned signals are governed by *density, Young's modulus, shear modulus, compressibility* (or *bulk modulus*), and *Poisson's ratio* of the medium through which the seismic pulse travels. Similarly, the GPR method depends on the contrast in *electrical conductivity, magnetic susceptibility,* and *dielectric properties* between the object and the host

medium. In an electrical survey, galvanic currents are sent into the earth through a pair of electrodes, and voltages through another pair of electrodes implanted in the earth are measured.

The magnetic and gravity methods measure how the existing earth's magnetic or gravity field is distorted by the presence of buried objects. The earth's magnetic field is distorted near a ferrous (i.e., steel) object that has a higher *magnetic susceptibility* than its host medium. Similarly, earth gravity is distorted by an object whose *density* is either higher or lower than its surroundings.

The following table summarizes the commonly-used geophysical methods and their usages applicable to environmental investigations:

Table 1. Geophysical Methods Applicable to Environmental Investigations

Method	*Mode*	*Applications*	*Intrusiveness*
Gravity	Passive	Geologic mapping, faults, cavities, fractures	None: portable instrument
Magnetic	Passive	Geologic mapping (particularly mafic rocks such as diabase dikes), USTs, pipelines, burial trenches, utilities	None: hand-held walkover
Seismic	Active	Bedrock topography, fractures, rock hardness	Planting many geophones, Impacts on ground
GPR	Active	Soil horizons, USTs, pipes, trenches, utilities	Towing sensor on ground
Electromagnetic	Active	Groundwater depth, soil moisture, acid plumes	None: hand-held walkover
Electrical	Active or Passive	Groundwater depth, soil moisture, fractures, acid plumes	Planting several electrodes, Injection of currents
Radioactive	Active or Passive	Geologic mapping, radioactive plumes	None

UST: Underground Storage Tank

Most of these methods also can be used in boreholes. Commonly used single-hole well-logging methods for environmental studies include the electrical, electromagnetic, and radioactive surveys. Methods using multi-holes may include cross-hole seismic method, and seismic, ultrasonic and electromagnetic tomographic methods. Some of these methods are still in the development stage and, thus, not commonly used.

The geologic host rock at LANL, the Bandelier tuff, is non-magnetic, dry thus non-conductive, and relatively homogeneous in the scale of targets within the SWMUs: therefore, the geologic background noise may be low at the site. Since the absolute instrumental sensitivity of modern geophysical sensors far exceeds typical ambient noise level, the detectability of the buried objects depends on the background geologic and cultural noise at the site.

Not all the methods listed in Table 1 are favorable to any site; seismic and electrical methods, for instance, may not be suitable for some SWMUs at LANL because of the unwanted mechanical

(seismic) impacts or injected electrical currents that may react with unknown target materials. In addition, hardware used for these methods must, even though relatively minor when compared with boring and drilling, contact with or disturb the ground surface, which requires frequent radiation checks and tedious decontamination processes for workers and instruments. In contrast, magnetic and electromagnetic methods can produce highly acceptable data qualities and quantities for certain sites with minimal intrusion. Under favorable geologic conditions, the GPR method, despite its somewhat heavy logistics and power demand, can provide high target resolutions with minor ground contact. Based on all these considerations on both the local geology and nature of targets at the three SWMUs under this project, we selected the three geophysical methods: magnetic, electromagnetic, and GPR methods. In the following sections, we present somewhat extended descriptions of these methods.

2.1 Magnetic Method

The magnetic survey detects variations, or anomalies, that deviate from the earth's main reference magnetic field. The main field amplitude ranges from about 30,000 gammas at the equator to about 60,000 gammas at the poles. At TA-49, the earth magnetic field found to be about 52,000 gammas (primarily a function of the geomagnetic latitude).

Local magnetic anomalies are attributable to the differences in magnetic susceptibility in geologic materials. Magnetic susceptibility is a basic material property and represents the degree of magnetization of a material placed in an external magnetic field. Magnetic susceptibility of a geologic material is proportional primarily to its content of iron-bearing minerals, principally magnetite, the most abundant magnetic mineral in the earth. Sedimentary rocks generally have very small magnetic susceptibility compared with igneous or metamorphic rocks, which tend to have higher magnetite content. In contrast, magnetic anomalies from a man-made structure (such as SWMUs) are entirely due to the content of steel material which is the most common metal product and, thus, likely found in most waste sites.

The earth's magnetic field changes with time. Of several temporal variations, the only concern for a survey that may last for a short duration is the diurnal variation that has a period of one day and a typical amplitude of about 30 gammas, except for during magnetic storms that typically occur globally on some summer days during which the amplitude can be much higher. The diurnal variation, occurring in unison over several hundred miles, is highly oscillatory and peaks around local noon time when the solar action on ionospheric currents is strongest. Field operators can easily recognize the onset of such variations by regularly repeating the measurement at a same spot, which should reproduce within an accuracy of a few gamma. If the measurements at a spot do not repeat and a magnetic storm is suspected, the survey should be recessed until the event passes.

For a large and long-duration survey, often a "base station" is established to record the temporal variation that is subsequently subtracted from the field data; this requires additional logistics and precision "time-tagging" of two magnetometers. For a small site survey involving less than, say, a few acres, base station is not often productive considering the additional field logistics and post processing requirements. Equally high-quality data can be obtained by restricting the survey time

to early mornings and late afternoons as well as by continuously checking the instrument repeatability.

Magnetometers are grouped in two types; vector and scalar magnetometers. Vector magnetometers, typically fluxgate or optical-pump types, are relatively complex instruments, produce multiple, vectorial data sets requiring a large storage device, and are mostly used for airborne surveys. Despite certain interpretational advantages, vector magnetometers are not convenient to operate, and thus are rarely used for environmental surveys.

Scalar magnetometers, typically the proton-precession type, measure the total amplitude and, therefore, do not depend on the sensor orientation with respect to the earth's magnetic field. The scalar instrument produces one value at each location. The instrument is light, fast, simple, and convenient for a one-man survey operation. Owing to its popularity, there exist excellent theoretical bases and interpretive methods for scalar data.

The instrument used at TA-49 is a proton precession magnetometer (EG&G Geometrics G-846) having a 1-gamma stationary instrument repeatability. Figure 2.1-1 shows a photograph of a typical survey crew. Also shown are two magnetic anomaly plots over a small (550-gallon) underground storage tank (UST). The magnetic data in this example are collected at two different sensor heights: 2 feet (left) and 5 feet (right). Notice that the peak or trough in the data does not necessarily coincide with the location of the UST; this offset depends on several factors including the geomagnetic latitude of the site, orientation of the tank, and the degree of permanent magnetization of the tank. The difference between the two data sets in this example is called the "vertical magnetic gradient." It often produces a sharper target image than the total field alone can. For this reason, the two-level survey was conducted at Area 4 and Area 11 to produce both the total field and vertical gradient anomaly maps.

2.2 Electromagnetic Method

Electrical conductivity is an inherent property of a material to conduct electrical current, and is measured in an SI unit of siemen/meter (S/m), or popularly in milli-siemen/meter (mS/m) for shallow environmental surveys. Its inverse is known as electrical resistivity and is expressed in an SI unit of ohm-meter. Variations in shallow earth conductivity are caused by changes in soil moisture content, conductivity of groundwater, thicknesses of overburden and vadose zones, and properties that can be related to lithology. In a microscopic sense, electrical conductivity of rock or soil depends on its mineral matrix, porosity, permeability, and fluids that fill the pore space.

Effective depth of exploration of an active electromagnetic system can be varied by changing either (1) the spacing between transmitter and receiver coils, or (2) frequency of the transmitted field. The first method is often referred to as the "geometrical sounding" method that involves several transmitter-receiver coil-spacings at a given location: the depth of exploration increases with the coil spacing. The two coils, although typically connected by an umbilical cord, are physically separate and thus require two operators. The second method is referred to as the "frequency sounding" method that involves changing the transmitter frequency at a fixed coil spacing: the

depth of exploration, often called "skin depth" under this method, decreases exponentially with the frequency for a given geologic condition. Because both coils are enclosed in a unit, one surveyor can operate the instrument. Theoretical and practical discussions on these methods may by found in Grant and West (1965), Keller and Frischkneckt (1966), Kaufman and Keller (1983), and Nabighian (1988).

Figure 2.2-1 (right), adapted from Won (1980), shows ranges of conductivity for typical earth materials and the relationship between the transmitter frequency and the skin depth. In general, sediments and sedimentary rocks have higher conductivity than igneous or metamorphic rocks. Clay, owing to its electrolytic interaction with water, exhibits high conductivity, while typical sand shows relatively low conductivity. In contrast, electromagnetic anomalies from a man-made structure (such as SWMUs) are entirely due to metals, including steel, that are likely found in most waste sites. Under favorable geologic conditions, the method can also detect leachate plumes that are electrically-conductive, acidic or alkaline.

Although there is a wide variety of active-source electromagnetic survey instruments, their operating principles are basically the same: a time-varying electromagnetic field is induced into the earth from a transmitter placed either on the surface or in the air, and the secondary induced field from the subsurface is measured by a receiver unit. Transmitter and receiver are often made of shielded pick-up coils. The secondary field is typically recorded in two parts; in-phase and quadrature (out-of-phase) components that are, for some commercial units, translated and displayed directly in earth conductivity values.

The basic principle of a frequency-domain electromagnetic system involves the measurement of change in mutual impedance between a pair of coils moving over the earth. A transmitter coil sets up a time-varying electromagnetic field that induces a system of currents within the earth below. This induced current, in turn, generates a secondary magnetic field that is measured by a receiver coil. The fundamental equations describing the magnetic field generated by a dipole located at or above the surface of a layered earth have been known to the geophysical community and will not be presented here. Some recent literature on electromagnetic methods are included in the references.

When the two coils are maximum-coupled (i.e., in a mutually co-planar or coaxial configuration), the primary field at the receiver coil is very strong compared to the magnitude of the secondary induced field. It is desirable to remove this large field, mainly to reduce the dynamic range needed for the receiver preamplifier circuit. This can be accomplished by using a third coil, commonly termed a "bucking coil," that is placed between the transmitter and receiver coils. The bucking coil is made so that its induced voltage from the primary field in the absence of the earth (i.e., in free space) is equal to that induced in the receiver coil. The bucking coil and the receiver coil are wired in opposing (or bucking) polarity. By eliminating the primary field, the combined sensor unit thus produces a zero output in free space. When a conductive body (e.g., a steel UST) is present nearby, the sensor produces a differential output depending only on the geometry and conductivity structure of the target and the earth.

The electromagnetic field is shifted in phase on encountering a relatively good conductor. This conductor becomes the source of the secondary field that differs in phase from the primary field, while having the same frequency. The secondary field and its phase relation with respect to the primary field are the main quantities recorded. The secondary field detected by the sensor is split into in-phase and quadrature (out-of-phase) components, which are expressed in ppt (parts-per-thousand) or ppm (parts-per-million) against the primary field strength that would have been induced in an unbucked receiver coil. This complex quantity (real and imaginary) is called the mutual coupling ratio, and it becomes the basis for subsequent data interpretation.

The electromagnetic survey for this project employed Geophex's new digital, multi-frequency electromagnetic unit (GEM-1). Figure 2.2-1(left) shows a photograph of a typical survey. Also shown is a GEM-1 anomaly plot over the same 550-gallon UST that was discussed in the previous section. Notice that, unlike the magnetic data, the peak in the anomaly data does coincide with the location of the UST; this is often the case, one of the advantages of this method.

GEM-1, a single-operator unit weighing about 8 pounds, transmits digitally constructed waveforms and measures the earth response automatically up to eight frequencies, each lasting about 0.1 second. The system is considered to be the most unique, advanced hand-held unit of this kind. Geophex developed and field-tested GEM-1 during 1989 and 1990 under research funding of the US Army. The prototype unit has been used by Geophex surveyors at many environmental sites. The results have been compared with data from other commercial instruments and with ground-truth data. Geophex is currently upgrading its hardware and software to produce a production model under a continued Army funding. The first production model is planned to be in service by early 1992.

GEM-1 has a typical sensitivity of about 10 ppm. This demonstrated sensitivity is at least an order-of-magnitude better than any existing portable electromagnetic sensors that are commercially available. In addition to its superb sensitivity, GEM-1 is capable of operating in multiple frequencies, which will aid in interpreting the measured anomalies in terms of the geometry and physical properties of the target. The multi-frequency transmission and interpretation capabilities are unique to this instrument.

Despite our claims of the technical superiority of GEM-1 over available commercial units, GEM-1 is presently non-commercial and, thus, the LANL staff are not likely to be familiar with its principle of operation. Appendix A describes technical motives of the development, theoretical aspects, and operating principles. Since the system is not commercial at this time, we request LANL to treat this document as a proprietary material of Geophex and use it for LANL's internal review only.

2.3 Ground-Penetrating Radar

This method employs an extremely short electromagnetic pulse that penetrates into the earth. A small portion of the pulse energy is reflected to the surface. The return signal is continuously recorded for a short duration on a strip-chart or, in some cases, into a digital recording device.

Amplitude of the reflected pulse depends primarily on the medium's dielectric constant. GPR anomalies result when there is a contrast in bulk dielectric property between materials, such as sedimentary formations having differing minerals and compositions. Dielectric constants of some typical materials are listed in Table 2.

Table 2. Dielectric constants of some typical materials

Material	Dielectric Constant
Air	1
Water	81
Soil (dry to moist)	4 - 30
Clay (dry to moist)	7 - 43
Sandstone (dry to moist)	4 - 12

For instance, there is a significant contrast in the dielectric property between clay and sandstone (or sand); owing to this contrast, GPR can usually detect a shallow clay horizon below a sand formation. In contrast, GPR anomalies from a man-made structure (such as SWMUs) result mostly from artificial geometric shapes of buried targets. These targets may include both metallic and nonmetallic objects such as drums, pipes, concrete blocks, bulk chemicals, animal bones, etc. Under favorable geologic conditions, the method can also detect disturbed soils and backfills.

The GPR employed for this survey is the SIR System-3 manufactured by GSSI, Inc. The system includes a Model PR-8304 Profiling Recorder; a GSSI Color Signal Processor and a color monitor; a transducer having center frequencies of 500 MHz; CC-30/11 Control Cable with a 30-m length; and a Model 10 Remote Marker. All instruments were powered by a 12 VDC battery from an automobile. Figure 2.3-1 shows a photograph of a typical survey. Also shown are two GPR profiles over the same 550-gallon UST that was discussed in the previous section. The geometry and size of the UST can be clearly inferred from the two mutually perpendicular profiles shown in this example.

A note of warning on GPR: the ability of GPR to detect buried objects is often over-rated. This is partially due to the fact that most profiles shown in published articles present only the successful ones (including the UST profiles in Figure 2.3-1!). Those successful ones render the uninformed an over-expectation toward the method, as well as an illusion that such resolutions can be routinely achieved. There are two inherent drawbacks in GPR: (i) the ability for an electromagnetic pulse emitted by a GPR to penetrate into a geologic medium is severely limited by the medium's electrical conductivity (causing rapid attenuation with depth) and physical inhomogeneity in soil (causing continuous back-scattering thus loosing energy), and (ii) GPR has a narrow-vision, particularly for shallow targets, and thus requires dense profile coverage. These two drawbacks, which are highly site-dependent and thus often unpredictable, make GPR one of the most finicky geophysical sensors.

3.0 Results

At each SWMU site, we first conducted a magnetic survey covering a large area that extends beyond the suspected wastes site. At Areas 4 and 11, both the total magnetic field and its vertical gradient data were obtained. At the Landfill site, however, only one-level total field magnetic data were obtained. The magnetic data were compiled in the field to determine the overall extent and nature of the buried wastes. Since the Bandelier Tuff is known to be non-magnetic, all observed magnetic anomalies must originate from buried steel objects within the waste sites.

Once the magnetically anomalous areas had been identified, we proceeded with the electromagnetic survey within the magnetically anomalous areas to further delineate the buried objects. The targets include all metal objects (steel, copper, aluminium, etc.) and possibly conductive leachate plumes. GEM for this survey was programmed to operate at transmitter frequencies of 800 Hz, 3,200 Hz, and 9,600 Hz. The skin-depth at 800 Hz exceeds 100 feet. In general, a strong in-phase anomaly indicates presence of good conductors while a strong quadrature anomaly indicates a less conductive medium. Since many small, isolated targets are scattered over a given SWMU site, rigorous interpretation of each anomaly is not attempted in this report. The anomalies are interpreted to the extent of locating these targets and determining their approximate geometries.

Finally, GPR surveys were conducted over selected magnetic and electromagnetic anomalies. The profiling covered about 3,000 linear feet during this survey. Recordings were made either on magnetic tapes in false-color image or on black-and-white electrostatic chart papers. Due to the data's 2-D nature, presentation of a large amount of GPR data in a technical report is unwieldy. To be practical, particularly in a highly heterogeneous area (such as a waste burial site), the GPR survey is best used in a "search-and-flag" mode that involves recording GPR anomalies on a site map as the survey progresses, while reviewing the records on the video monitor. Therefore, the presentation of GPR data in this report is limited to only one exemplary profile in Area 4. All other anomalies are directly incorporated in the final interpreted site map as discussed below.

The end-product of the survey for each SWMU is presented as an "interpretive sketch" showing all suspected buried objects in a single map that may somewhat resemble archeological drawings. The sketch incorporates all geophysically inferred objects as well as exposed structures such as concrete pads, metal posts, fences, etc. Geometries associated with the inferred objects in this sketch are the best approximations based on the geophysical data. We hope that such an "interpretive sketch" map can serve a good starting point for a site characterization process. The map can be used for (i) further detailed geophysical surveys; (ii) a guide for boring, drilling, and sampling; (iii) planning of future corrective actions; and/or (iv) a basis for a long-term compliance monitoring plan.

For the rest of this section, we present the results of geophysical investigation for each SWMU in the order of Area 4 (Test Shafts), Area 11 (Leach Field), and Landfill/Trash-Burning Area.

3.1 Area 4 (Test Shafts)

The magnetic survey covers a rectangular area of 220 feet by 140 feet at a survey grid of 10 feet. The field was measured at two sensor heights of 2 feet and 5.3 feet (difference is about 1 m) to derive a vertical gradient map. Figure 3.1-1 shows the total field measured at 5.3 feet. The background magnetic field in this map is 51,600 gamma (i.e., the measured field is 51,600 gamma plus the number at each data point shown in the map). A 3-D fish-net diagram of the data is also shown in the figure as a visual aid.

Exposed concrete patches and metal pipes are also indicated in the map. Notice that there appears to be no disturbance beyond an "Indian mound" to the northwestern portion of the site. With some exceptions, magnetic anomalies correlates well with the exposed concrete patches, although the size of a patch does not necessarily seem to be proportional to that of the magnetic anomaly. Figure 3.1-2 shows a vertical magnetic gradient map that defines anomalous areas with improved lateral resolutions.

Figure 3.1-3 shows the in-phase and quadrature electromagnetic anomaly maps at 800 Hz. The survey area is the same as that of magnetics minus 4 northernmost lines where no magnetic anomalies were identified and, thus, considered undisturbed. As a visual aid, a net diagram for the 800-Hz in-phase anomaly is shown in Figure 3.1-4. Figures 3.1-5 and 3.1-6 show similar maps at 3,200 Hz and 9,600 Hz, respectively. In comparison with magnetic data, an electromagnetic anomaly is commonly centered over the target; therefore, electromagnetic data are often superior in locating and bounding the lateral extent of a conductive target. Tightly-bunched contour lines, particularly for the in-phase data, often correspond with the lateral edges of a target. The contour-bunching generally becomes tighter with an increasing source frequency. We note several well-defined electromagnetic anomalies that are co-located with magnetic anomalies. In addition, a few anomalies are new and were not seen before in the magnetic data.

Figure 3.1-7 shows a typical GPR profile in Area 4. The profile crosses several pipe-like objects and a concrete patch. About 30 such profiles were obtained in the southern half of Area 4. Finally, all three geophysical data sets (i.e., magnetic, electromagnetic, and GPR) were used to derive the interpretive sketch map shown in Figure 3.1-8. This map shows all significant, geophysically-inferred, buried objects as well as exposed structures such as concrete patches and pipes.

3.2 Area 11 (Leach Field)

The magnetic survey in Area 11 covers a rectangular area of 290 feet by 180 feet at a survey grid of 10 feet. The field was measured at sensor heights of 2 feet and 5.3 feet to derive a vertical gradient map. Figure 3.2-1 shows the total field measured at 5.3 feet. The background magnetic field in this map is 52,000 gamma (i.e., the measured field is 52,000 gamma plus the number at each data point shown in the map). A 3-D fish-net diagram of the data is also shown in the figure as a visual aid. The map shows several surface features such as a culvert (near the gate), sign posts (middle; corresponding to the suspected chemical leach field), two vertical 1-ft diameter truncated shafts

(west), and a small segment of a horizontal pipe (northeast). Magnetic data clearly indicate that the disturbance is limited to the central portion of the survey area. Figure 3.2-2 shows a vertical magnetic gradient map of the site.

Two major magnetic anomalies are those caused by the culvert and two steel shafts. The anomaly at the steel shafts continues westward indicating that there may be more unexposed shafts. The rest of the minor anomalies are accounted for by sign posts and a small pipe segment. Consequently, we conclude, from the lack of unaccounted magnetic anomalies, that there are no significant steel objects under the suspected leach field.

The electromagnetic survey was conducted in a smaller rectangular area (200 ft x 90 ft) as shown in Figure 3.2-1. Figures 3.2-3, 3.2-4, and 3.2-5 shows the in-phase and quadrature electromagnetic anomaly maps (along with 3-D net-diagrams for in-phases only) at 800 Hz, 3,200 Hz, and 9,600 Hz, respectively. Two conspicuous oval-shaped anomalies occur at all frequencies in the central portion of the survey area near the two sign posts. East-west irregularities to the south in the quadrature anomalies (particularly at 800 Hz) have been determined to be from an instrument malfunction and should be disregarded. The two oval-shaped anomalies cover an area of about 60 ft by 50 ft, or about 3,000 sq-ft.

Several experimental GPR profiles were run over the culvert (buried at 2-3 feet deep) near the gate. In all cases, this culvert was clearly identifiable from the GPR records. The central portion of the survey area was then covered by many additional GPR lines. Numerous pipe-like objects were identified over the alleged leach field. About 20 feet south of the culvert along the gravel driveway, GPR encountered a strong, extensive, planar reflector at about a 2-ft depth; since neither magnetic nor electromagnetic data indicate anything anomalous here, we conclude that the feature is likely due to the compaction of the gravel driveway. GPR data to the west over the suspected, additional steel shafts area (based on the magnetic data) indicated a few small trench-like, disturbed soil zones that may correspond with the tops of the buried pipes. Unfortunately, the GPR profiles at that time were monitored on a color CRT screen and recorded only on the magnetic tape without paper charts. The tape can be presented to LANL, if desired.

Since the two oval-shaped anomalies have no corresponding magnetic anomaly, we can safely preclude any extensive steel structures beneath the area. By default, the anomalies can be caused by a hypothetical structure made of non-ferromagnetic metals (copper, stainless steel, etc.). Since the area is known to be the approximate location of the leach field, however, the more likely explanation is that it represents the areal extent of the chemical leachate plume that is highly conductive. We do not have any good explanation at this time of why the plume appears to be divided in half. A revisit by a GPR survey may reveal a certain structural division (e.g., concrete wall) in the middle of the plume.

Finally, all three geophysical data sets (i.e., magnetic, electromagnetic, and GPR) were used to derive the interpretive sketch map shown in Figure 3.2-6. This map shows all significant, geophysically-inferred, buried objects as well as exposed structures. The oval-shaped anomaly is tentatively labeled to be the chemical leach field.

3.3 Landfill/Trash-Burning Area

The magnetic survey in this area covers a rectangular area of 490 feet by 160 feet at a survey grid of 10 feet. The total field was measured at a sensor height of 6 feet. Gradient data were not considered necessary since the main purpose was locating the boundary of the landfill rather than delineating its content. Figure 3.3-1 shows the total field. Also shown are the four metal poles (connected by a dotted rectangle having a dimension of about 200 ft by 35 ft) that presumably define the landfill boundary. The background magnetic field in this map is 52,200 gamma (i.e., the measured field is 52,200 gamma plus the number at each data point shown in the map). A 3-D fish-net diagram of the data is also shown in the figure as a visual aid. Because additional burial was suspected the magnetic survey continued almost to the cliff edge to the north. Magnetic data clearly indicate that the trench continues another 150 feet or so to the north (see the net-diagram in Figure 3.3-1). The additional trench appears to be in line with and a continuation of the known one.

The electromagnetic survey was conducted in a smaller rectangular area (250 ft x 100 ft) as shown in Figure 3.3-1. Figure 3.3-2 shows the in-phase and quadrature electromagnetic anomaly maps of the site at 800 Hz. As a visual aid, a net diagram for the 800-Hz in-phase anomaly is shown in Figure 3.3-3. Figures 3.3-4 and 3.3-5 show similar maps at 3,200 Hz and 9,600 Hz, respectively. We note several well-defined electromagnetic anomalies that are co-located with magnetic anomalies. The electromagnetic data, in particular, indicate that the trench boundary defined by the four metal poles is fairly accurate, although the trench does continue to the north as manifested by the magnetic data.

The trench area denoted by the four poles was covered by numerous GPR profiles in an attempt to locate the trench boundaries. None of the profiles showed the boundaries. Based on additional trials elsewhere (see footnote 1), we tentatively conclude that the fill cover of this landfill exceeds 4 feet or so in thickness. A lower frequency antenna may be able to penetrate deeper. In addition, different GPRs with advanced wavelet-processing capability may be worth testing at this site. The reason for such a severe attenuation of an electromagnetic pulse through the Bandelier Tuff material (despite its dryness and thus low conductivity) has not been established.

Finally, all geophysical data sets (magnetic and electromagnetic) were used to derive the interpretive sketch map shown in Figure 3.3-6. The inferred trench has a dimension of about 330 ft by 35 ft, about 130 feet longer that the length denoted by the four metal poles.

---

1. Toward the end of the field work, we visited several exposed culverts and bridge deck locations in the vicinity of the LANL complex in order to determine the GPR's maximum potential depth of detection for such structures that appear to be buried in crushed Bandelier Tuff material. Most culverts at depths of 2 - 3 feet were detectable. However, any structures deeper than about 4 feet were not detectable by this GPR.

4.0 Conclusions and Recommendations

Geophysical requirements for the investigation of many environmental sites (particularly DOE's) are relatively new problems and call for innovations and improvisations. Considering the total amount of field effort in terms of the duration and cost, we believe the intent of this contract has been accomplished. As a part of strategy, we selected the least intrusive geophysical tools and survey modes in order to facilitate the field work, to minimize the costly decontamination procedures, and yet to maximize the amount of information derived from the survey. Such a strategy must be carefully designed particularly for those SWMUs with potential chemical and radioactive wastes. Without such a strategy, the work may last too long, becomes too costly, and may pose unnecessary risk to site workers.

The "interpretive sketch" map can be an intelligent starting point for a RCRA site characterization (SC) process, particularly for the preliminary site assessment (PSA) phase. The map represents a "preliminary assessment" of all major "symptoms" of each SWMU investigated. The map can be used for (i) further detailed geophysical surveys (in a reduced grid size, for instance); (ii) a guide for boring, drilling, and sampling; (iii) planning of future corrective actions; and (iv) a basis for the compliance monitoring plan.

Based on experience we gained from this pilot study, we present the following observations and tentative conclusions:

- Geophysical methods applicable to the initial investigation of LANL SWMUs must be as non-intrusive as possible, yet is able to produce large amount of data that can guide subsequent characterization. This non-intrusiveness is both to minimize workers' exposure to radioactive or chemical wastes and to reduce the decontamination processes required for people and hardware.

- Based on this pilot study, we conclude that the magnetic and electromagnetic methods meet the above conditions. These methods provide a rapid areal coverage, a large amount of reconnaissance data, and cost effectiveness. Once the methods have identified target areas, additional magnetic and electromagnetic surveys may be run in a tighter survey grid. At this time, GPR can be an excellent tool to be used in a "search-and-flag" mode. We recommend GPR not as a large area reconnaissance tool, but only when a target area is sufficiently delineated by magnetic or electromagnetic methods.

- Seismic (refraction or reflection) and electrical methods are not recommended during the early phase because of their intrusive nature (geophones, shot-holes, electrodes, etc.) and potential interactions with unknown wastes either through mechanical impacts or electrical currents. As the site characterization proceeds, thus with an increasing understanding of the site and confidence on its contents, additional geophysical methods may be evaluated for their applicabilities. At this time, additional GPR, electrical or other methods may become increasingly viable tools.

- When or if a site characterization proceeds to the point of advancing drill holes, an evaluation of applicability of various well-logging methods (magnetic, electromagnetic, natural radioactivity, acoustic televiewer, downhole camera, etc.) may be made. If multiple holes are available, cross-hole seismic, ultrasonic, or electromagnetic tomographic methods may be considered. We do not recommend drilling holes solely for the purpose of well-logging.

- Additional research on the applicability of the GPR to the LANL site-specific geologic environ may be justified to study the nature of the severe attenuation we encountered during this study. It appears that the attenuation is common to the Bandelier Tuff and its crushed aggregates. If the attenuation can be physically understood, an alternative strategy may be formulated. The approach may include a lower antenna frequency, advanced antenna configurations, and digital wavelet-processing technique. There are two commercial GPRs known to us, which may be able to increase the depth of exploration without down-grading the resolution.

References

Grant, F.S. and West, G.F., 1965, *Interpretation Theory in Applied Geophysics,* McGraw-Hill, New York, 584 p.

Kaufman, A.A. and Keller, G.V., 1983, *Frequency and Transient Soundings,* Elsevier Publishing, Amsterdam, 685 p.

Keller, G.V. and Frischkneckt, F.C., 1966, *Electrical Methods in Geophysical Prospecting,* Pergamon Press, New York, 517 p.

Nabighian, M.N., 1988, *Electromagnetic Method in Applied Geophysics, v. 1,* Edited by M.N. Nabighian, Society of Exploration Geophysicists, Tulsa, 513 p.

Telford, W.M., Geldart, L.P., Sheriff, R.E., and Keys, D.A., 1976, *Applied Geophysics,* Cambridge University Press, 860 p.

Won, I.J., 1980, A Wideband Electromagnetic Exploration Method - Some Theoretical and Experimental Results, Geophysics, v. 45, no. 5, pp. 928-940.

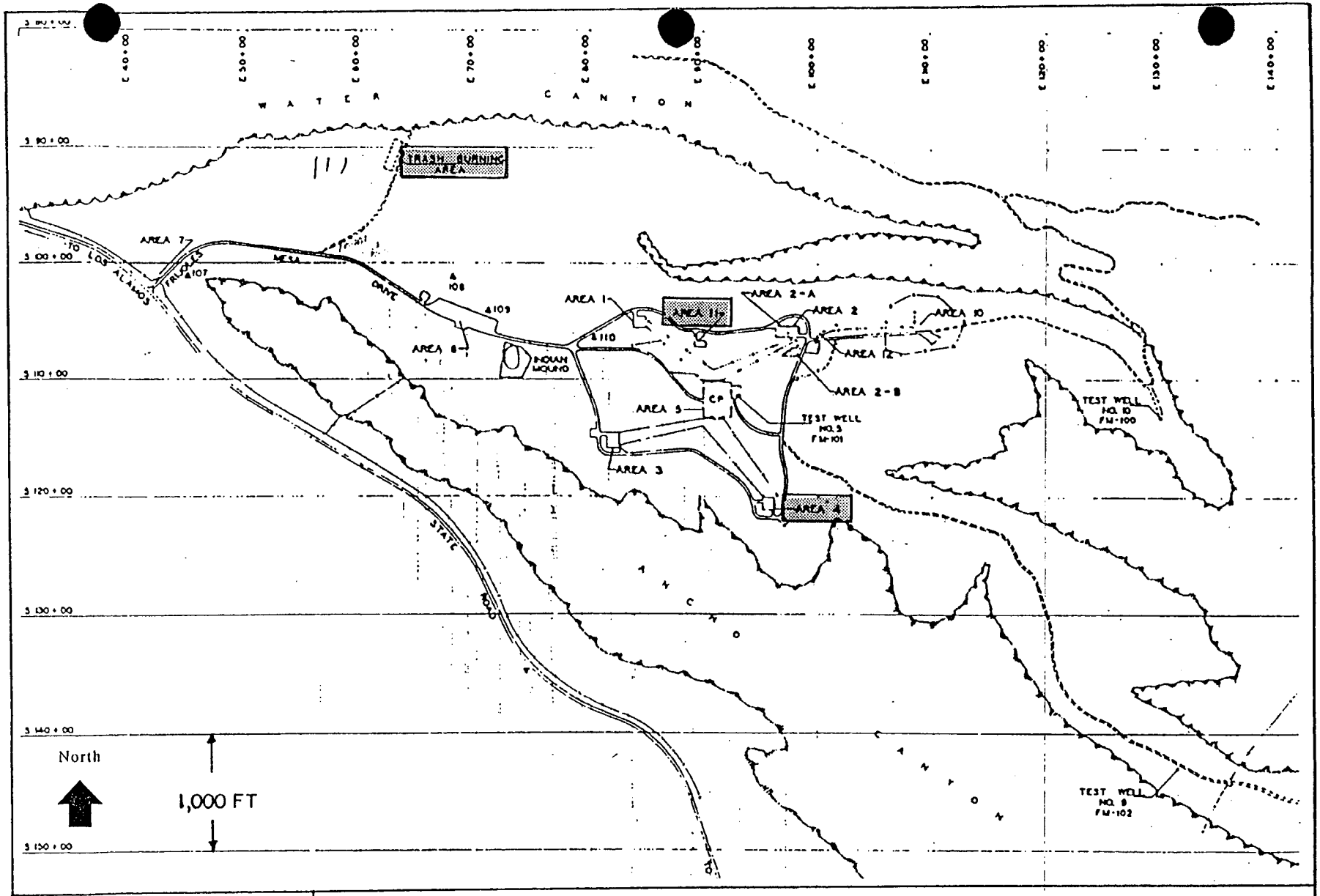

Geophex

Figure 1.0-1. Areal map of TA-49, Los Alamos National Laboratory.

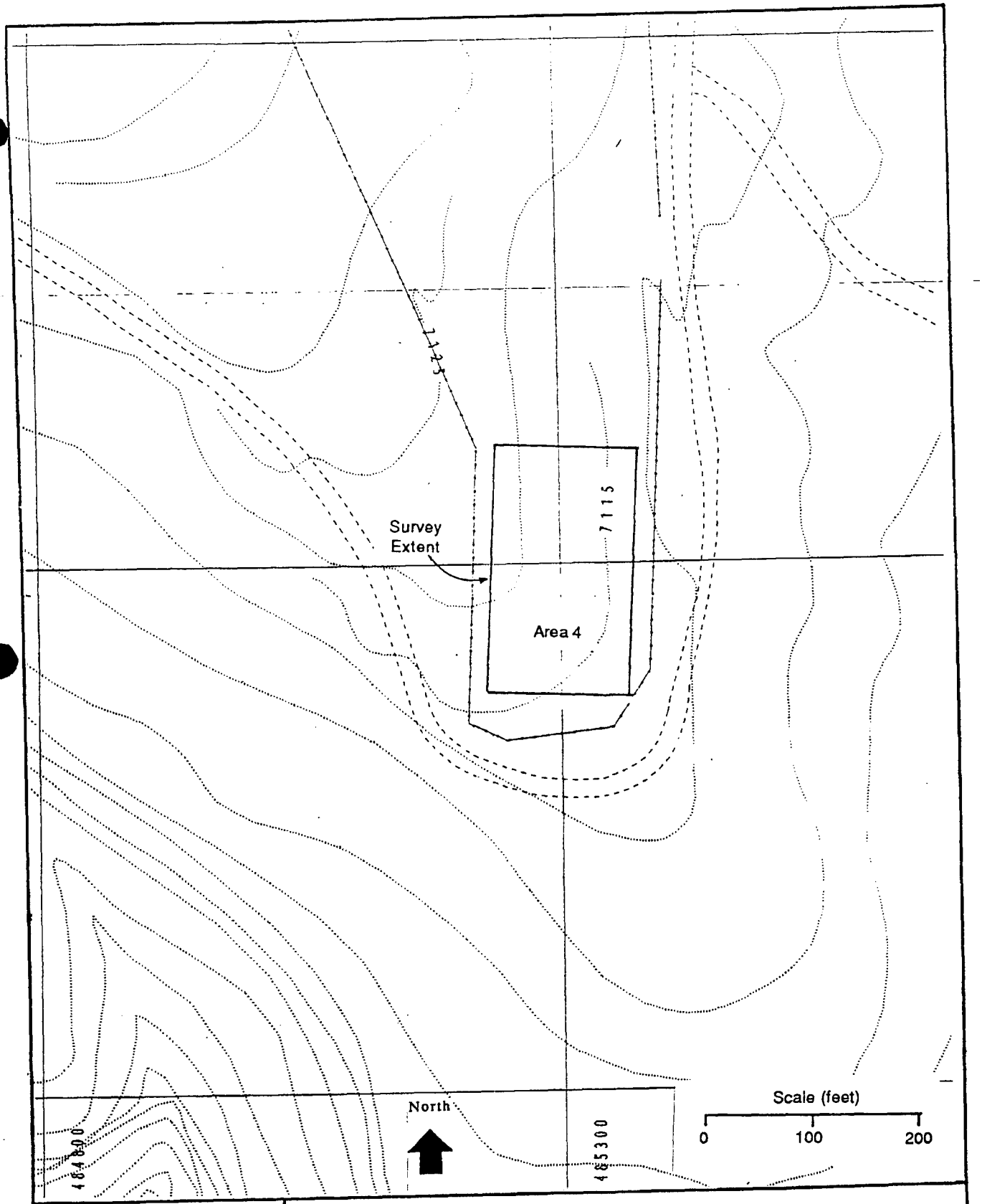

Geophex

Figure 1.0-2. Site map of Area 4 (Test Shafts).

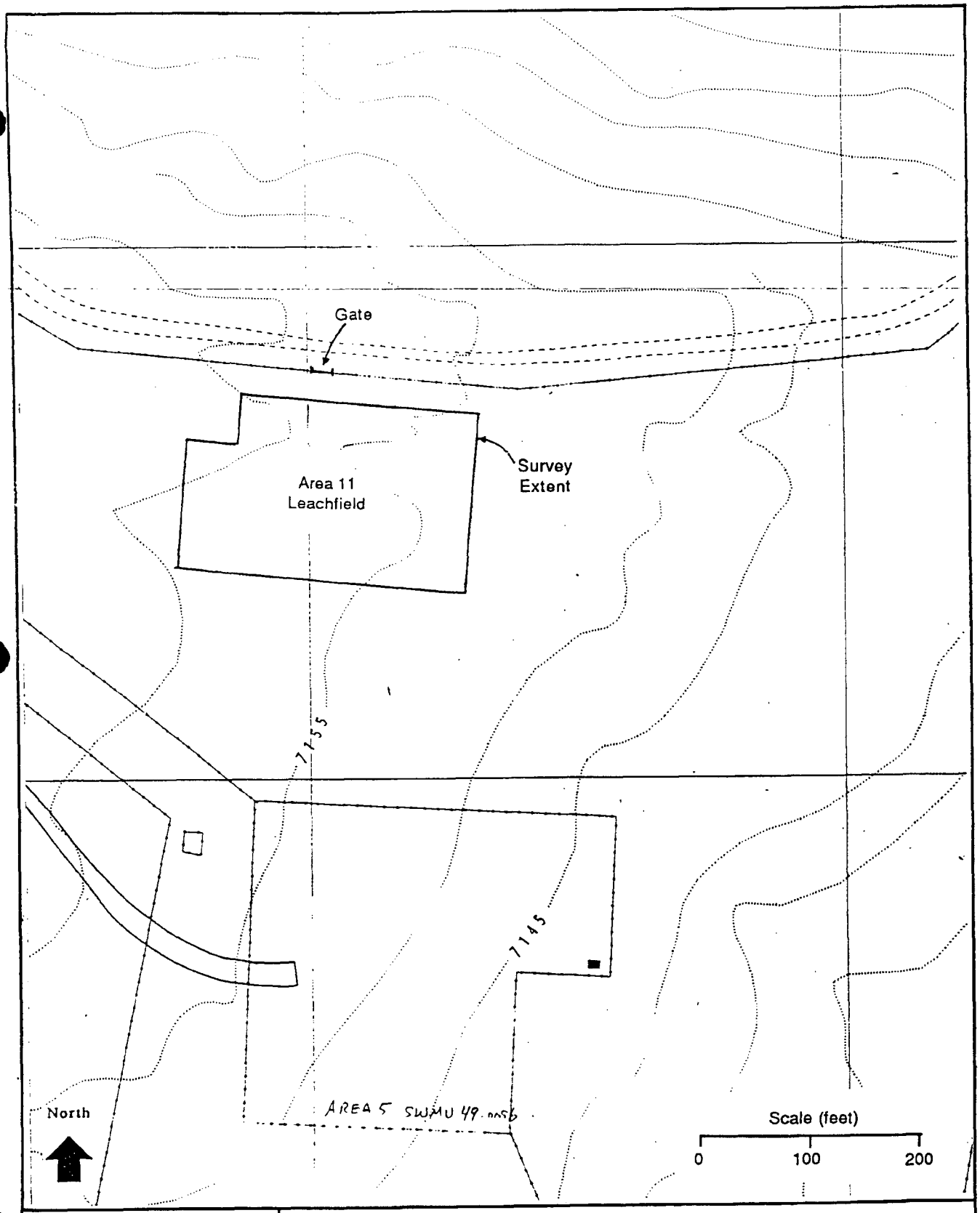

Geophex

Figure 1.0-3. Site map of Area 11 (Leach Field).

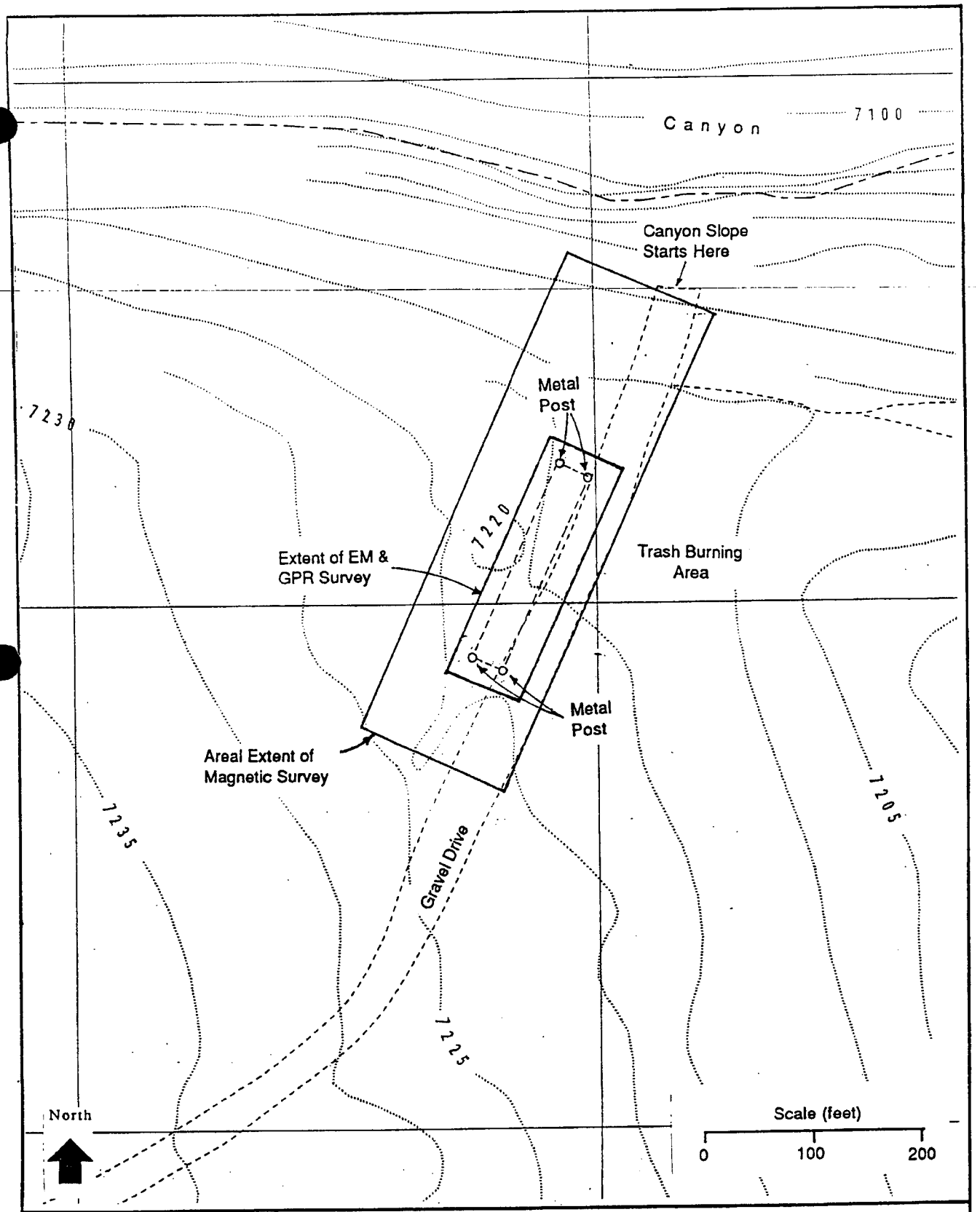

Geophex

Figure 1.0-4. Site map of Landfill.

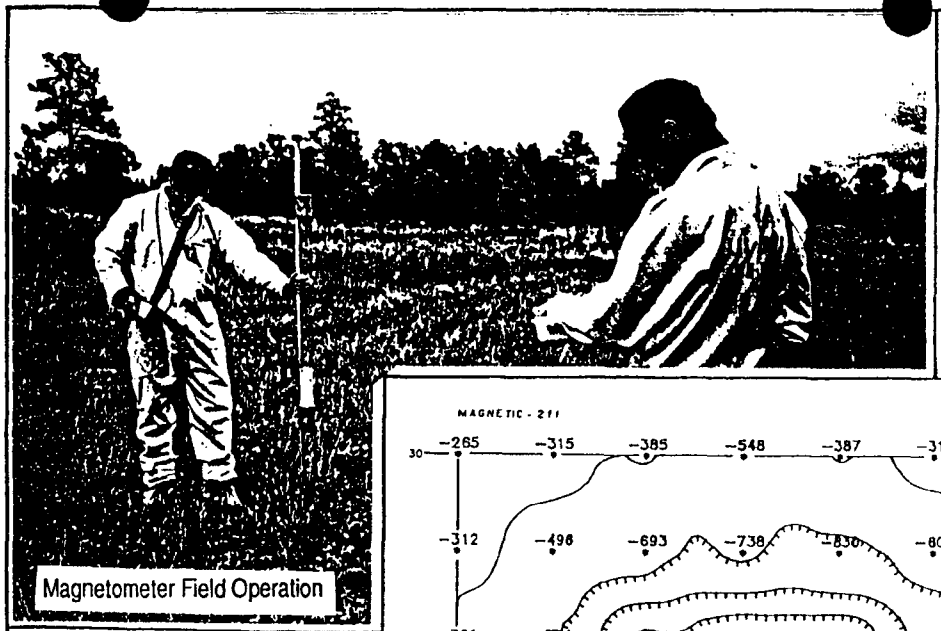

Magnetic Anomaly Maps Due to a 550-gal Underground Storage Tank (shaded rectangles).

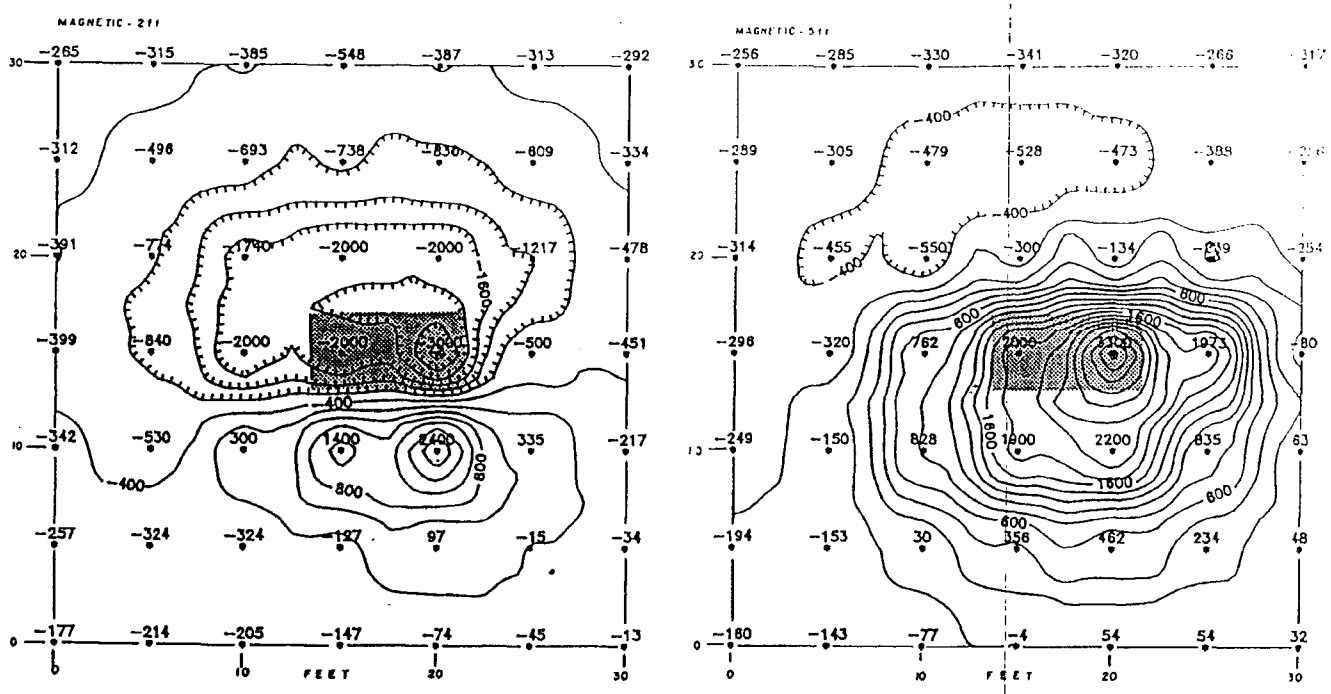

Sensor Height:	2 feet
Contour Interval:	400 gamma
Background Earth Field:	53,000 gamma

Sensor Height:	5 feet
Contour Interval:	200 gamma
Background Earth Field:	53,000 gamma

Geophex

Figure 2.1-1. Photograph of magnetic survey and two example contoured magnetic maps over an underground storage tank. The sensor height is 2 feet (left) and 5 feet (right).

800-Hz Inphase Anomaly over a 550-gal Underground Storage Tank (shaded parallelogram).

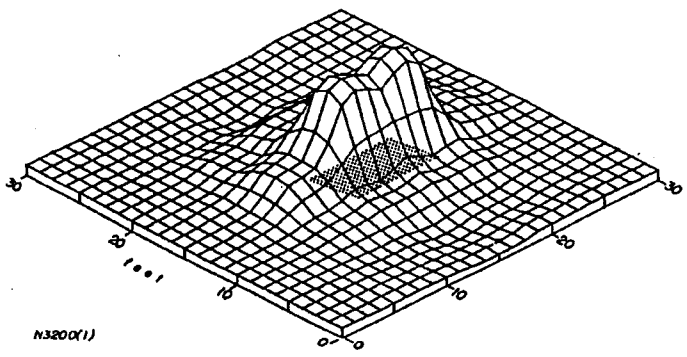

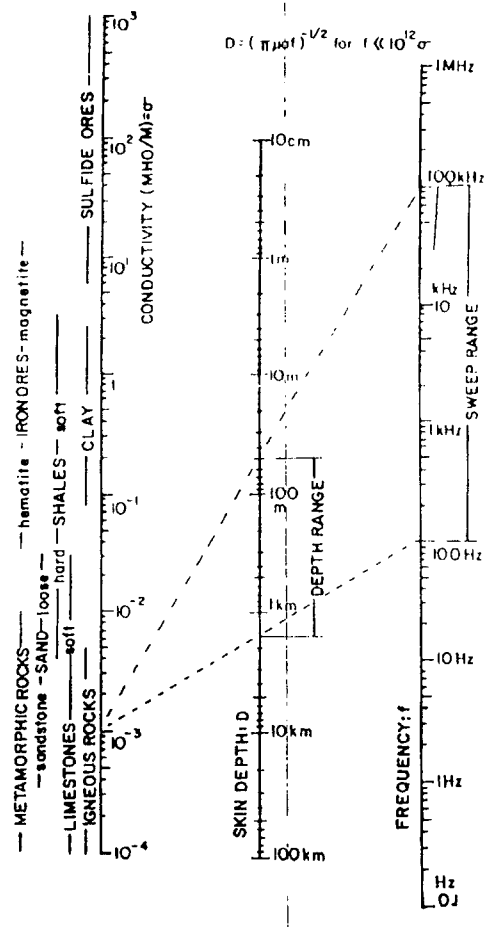

FIG. 1. Nomogram showing the relationship between source frequency, ground conductivity and depth of penetration (skin depth). A broadband or sweep-frequency EM with a frequency range from 100 Hz to 100 kHz would have a depth of exploration ranging from about 40 to 1500 m. (From Won, 1980.)

Geophex

Figure 2.2-1. Photograph of electromagnetic survey; an example EM anomaly over a UST (paralellogram). Also shown to the right is a nomogram showing the relationship between source frequency, ground conductivity, and depth of penetration (skin depth).

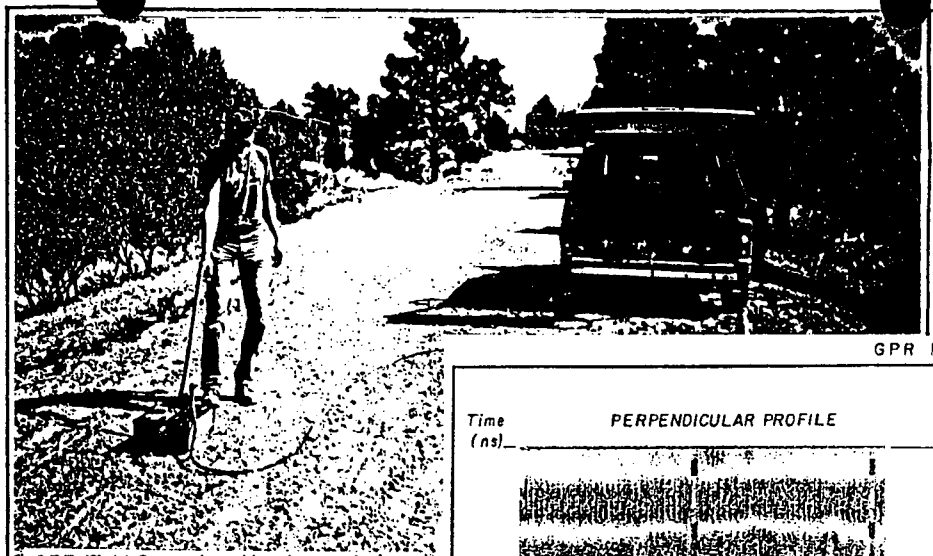

GPR Field Operation: Hand-operated 500 MHz Sensor and Recorder (in Truck)

Two 500 MHz GPR Profiles over a 550-gal Underground Storage Tank.

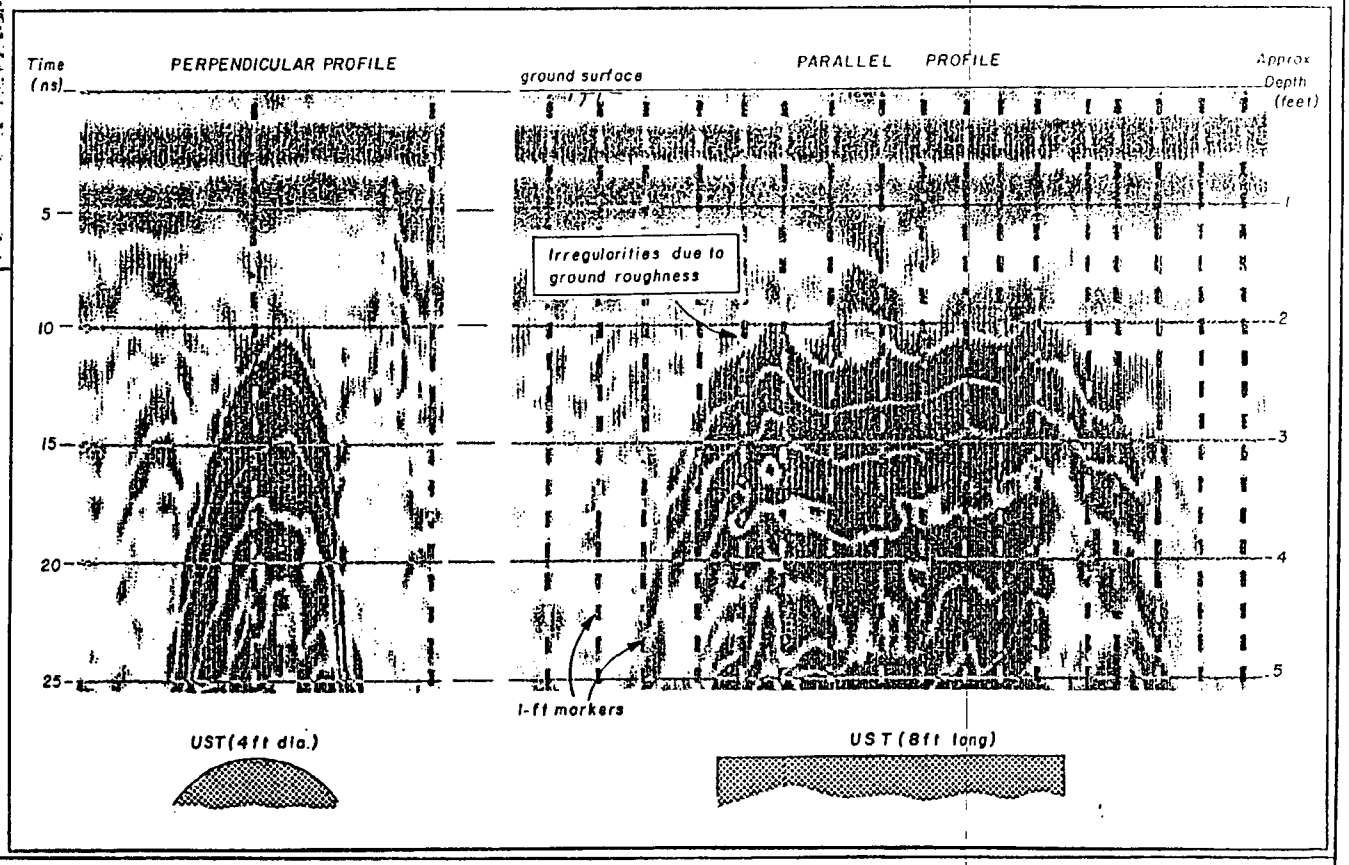

Geophex

Figure 2.3-1. Photograph of GPR survey and two GPR records over a UST.

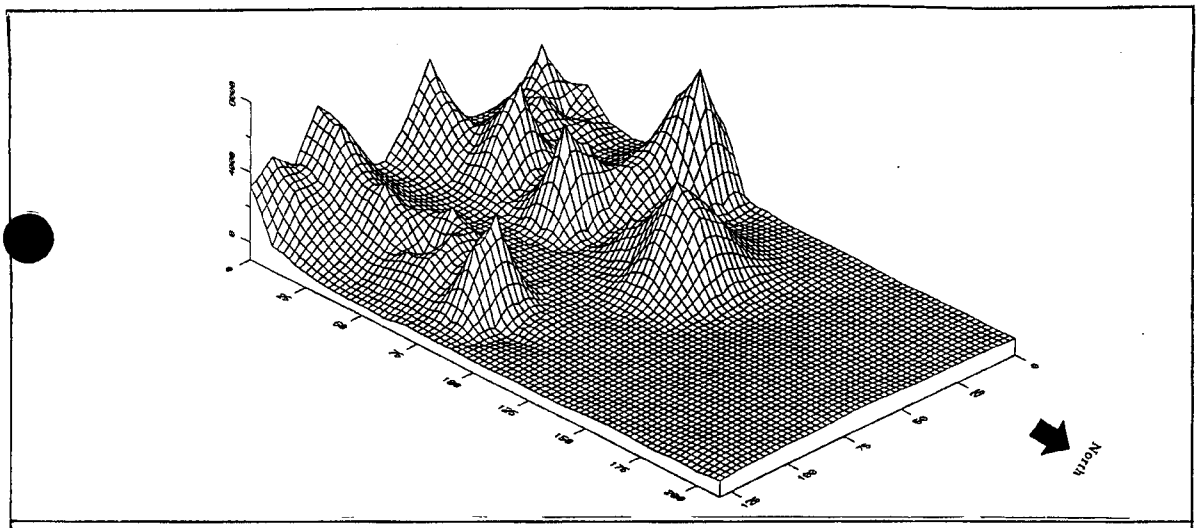

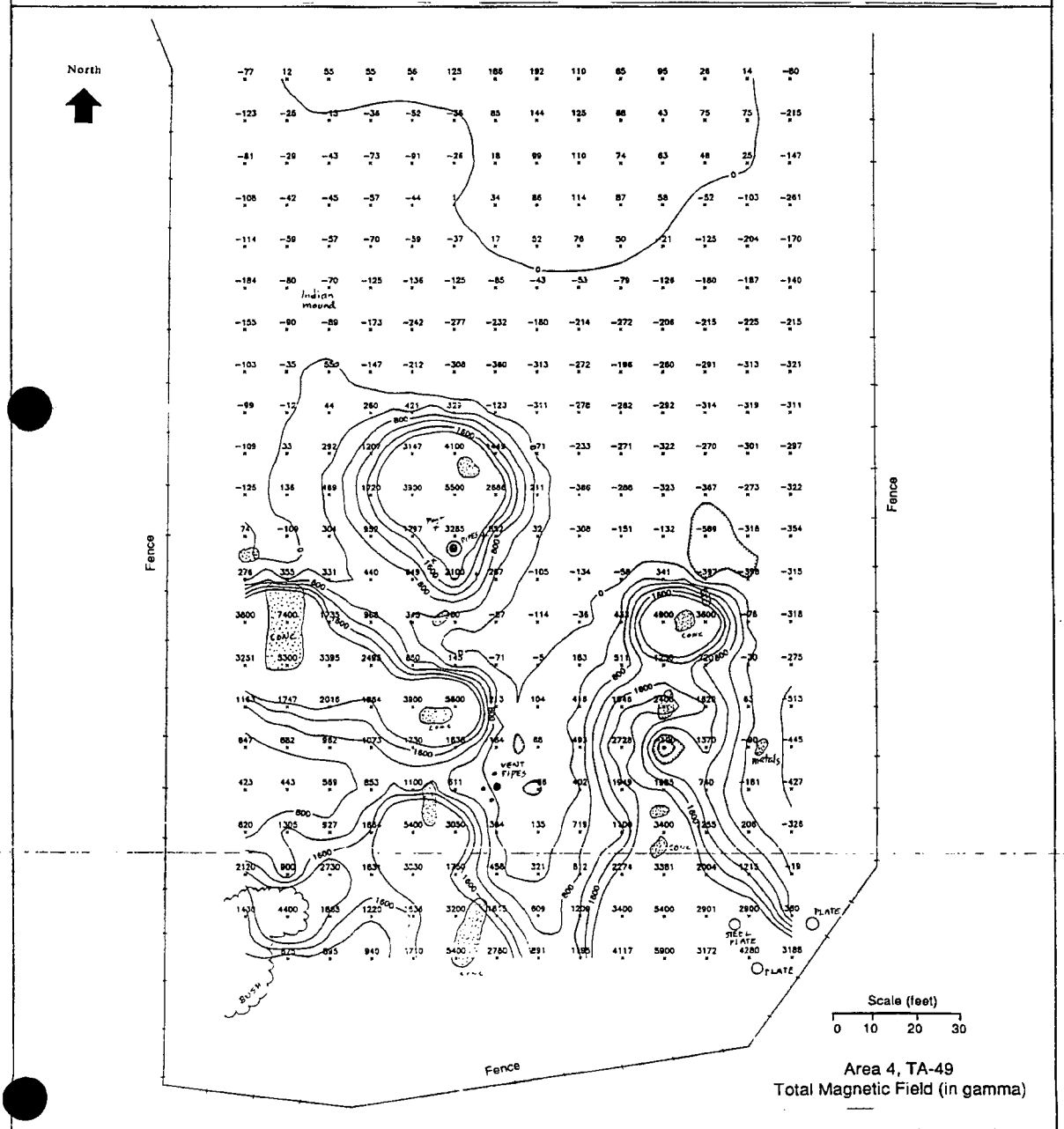

Geophex

Figure 3.1-1. Area 4 (Test Shafts): total field magnetic map (in gamma); Background = 51.600 gamma; Contour interval = 400 gamma.

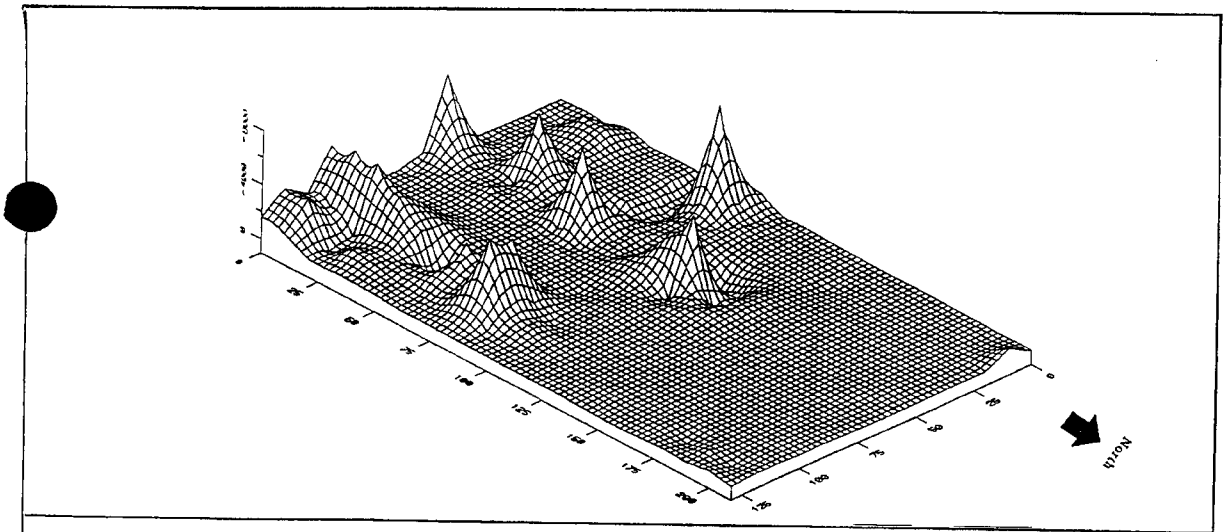
North

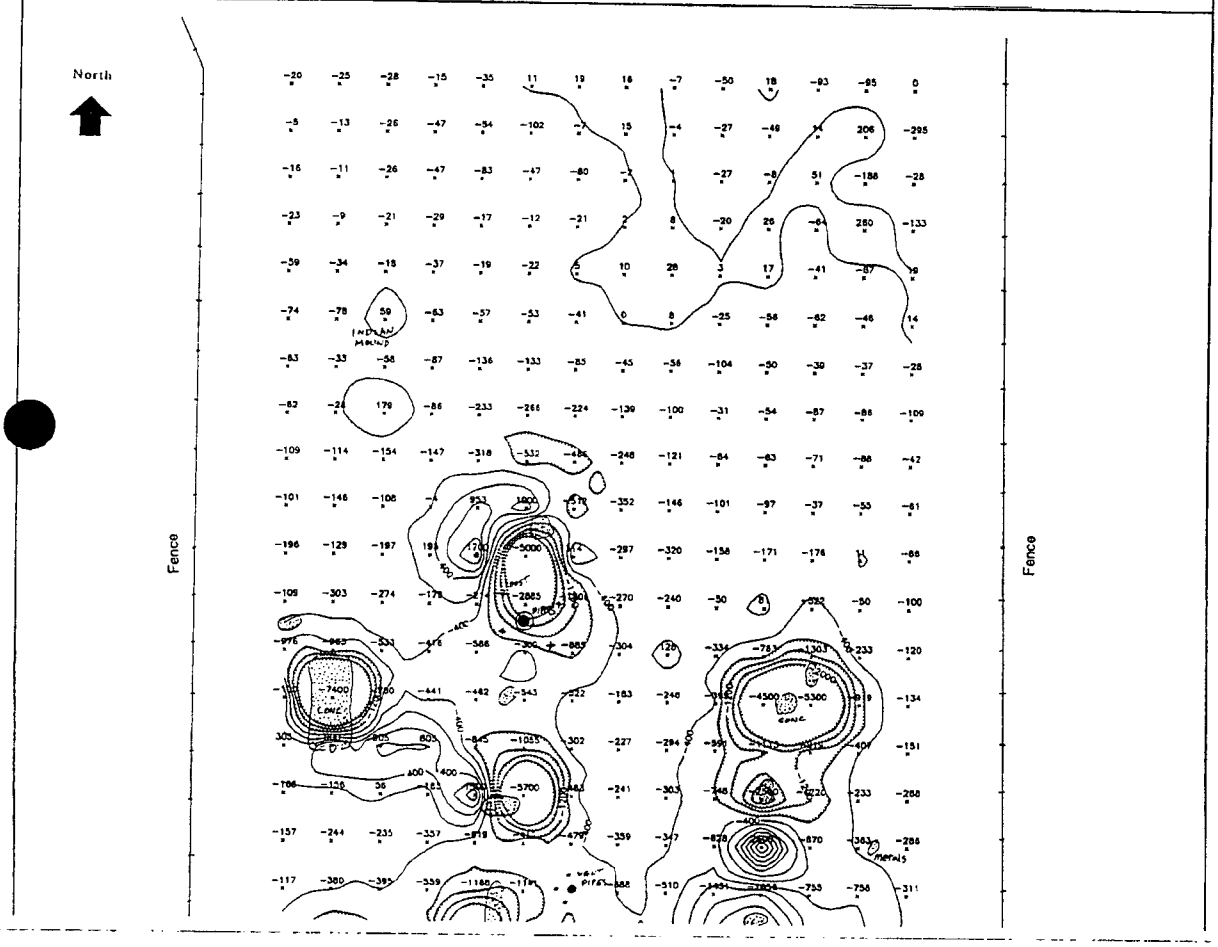
North
Fence
Fence
INDIAN MOUND
CONC
CONC
METALS

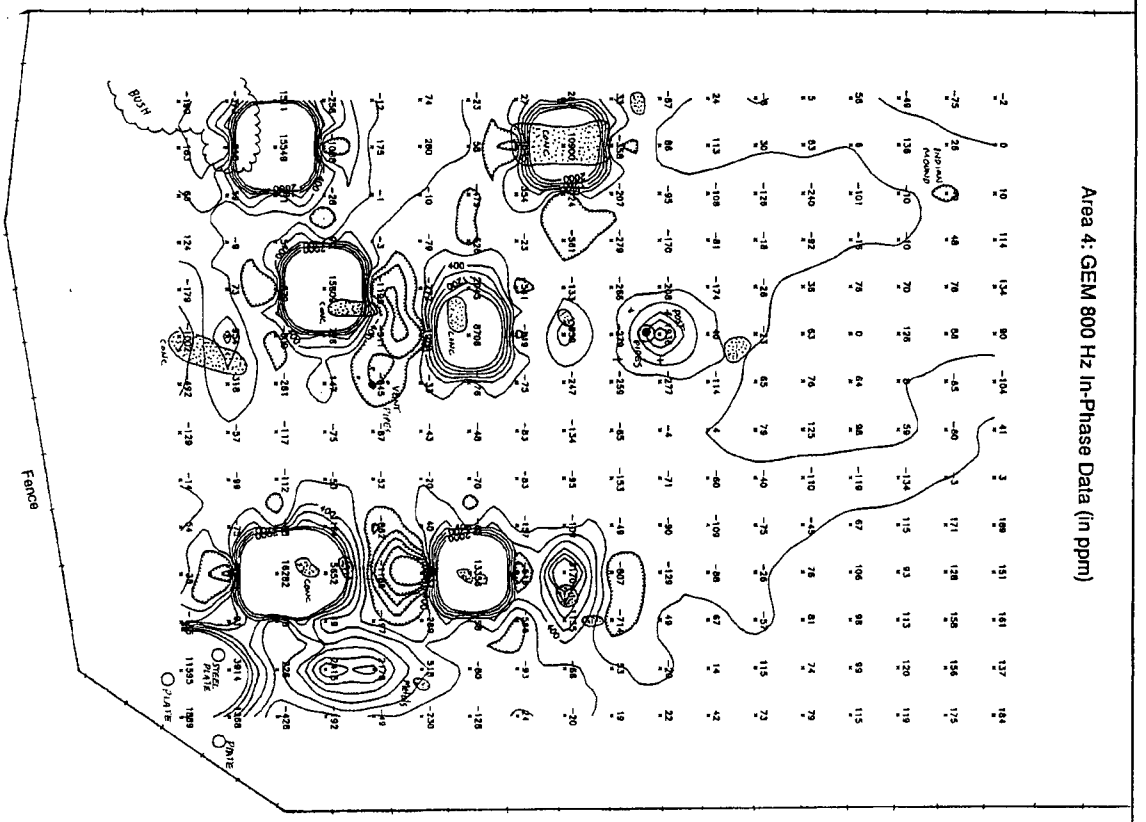

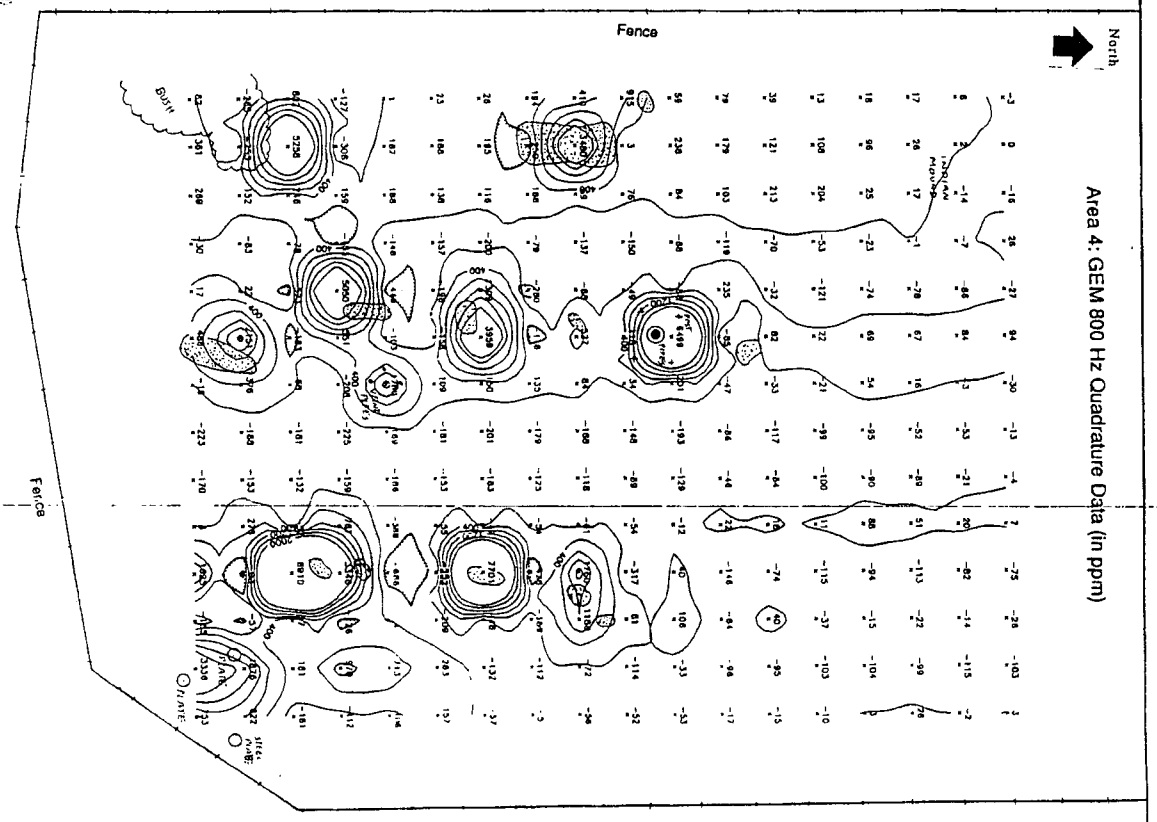

Geophex

Figure 3.1-3. Area 4: Electromagnetic data (in ppm); 800 Hz; Contour interval = 400 ppm.

Area 4: GEM 800 Hz In-Phase Data (in ppm)

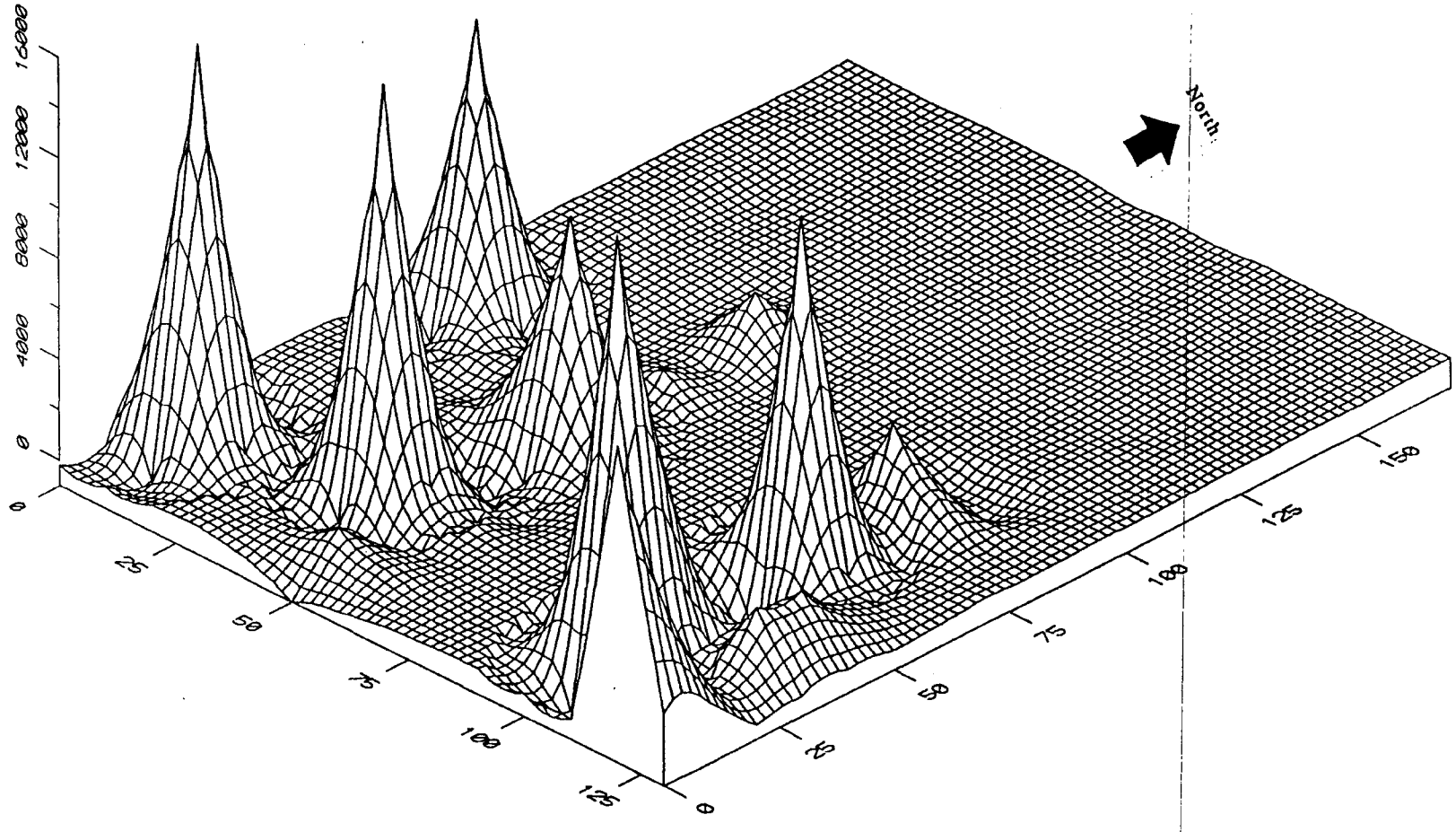

Geophex

Figure 3.1-4. Area 4: Fish-net view of electromagnetic data (in ppm); 800 Hz Inphase.

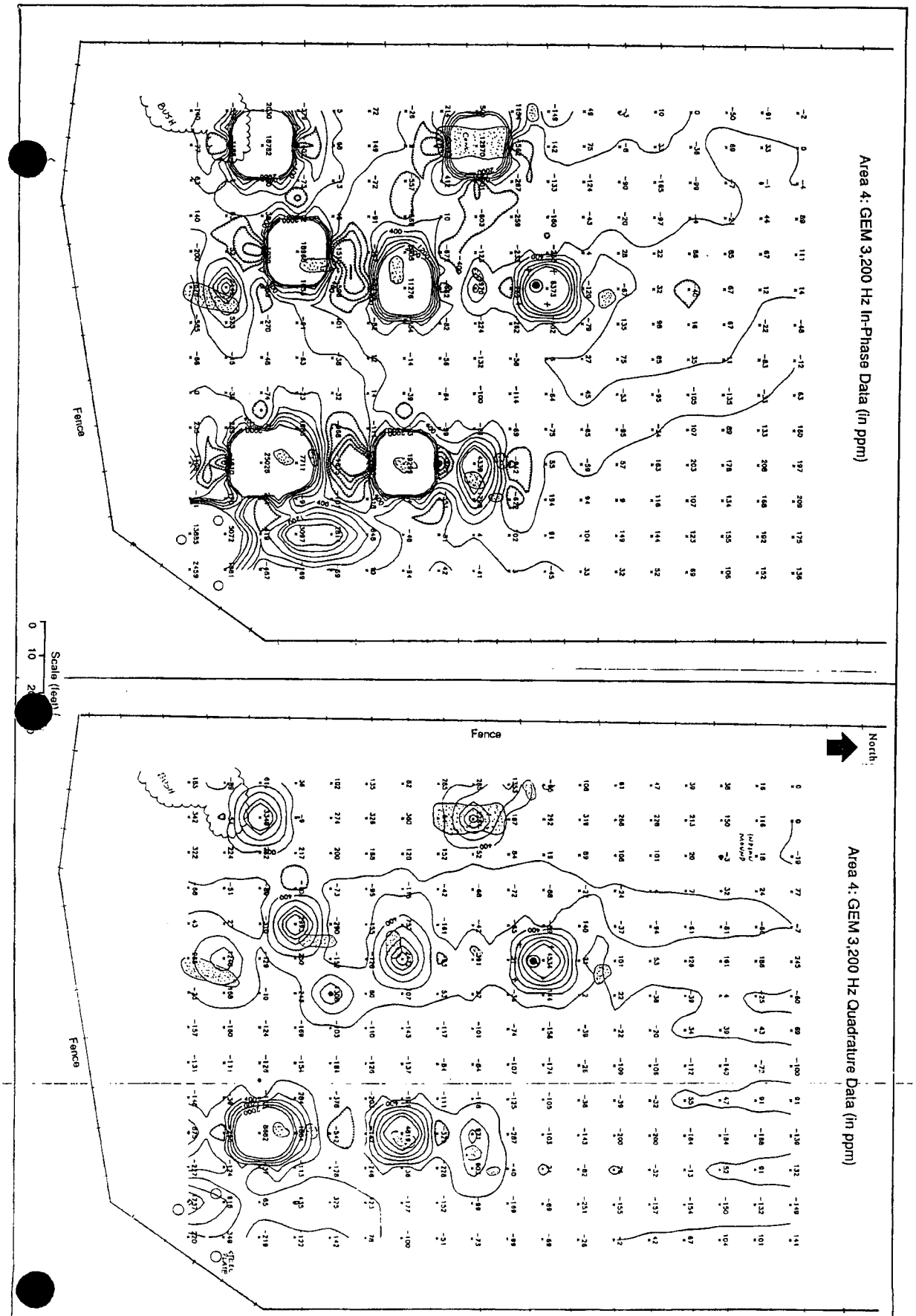

Geophex

Figure 3.1-5. Area 4: Electromagnetic data (in ppm); 3,200 Hz; Contour interval = 400 ppm.

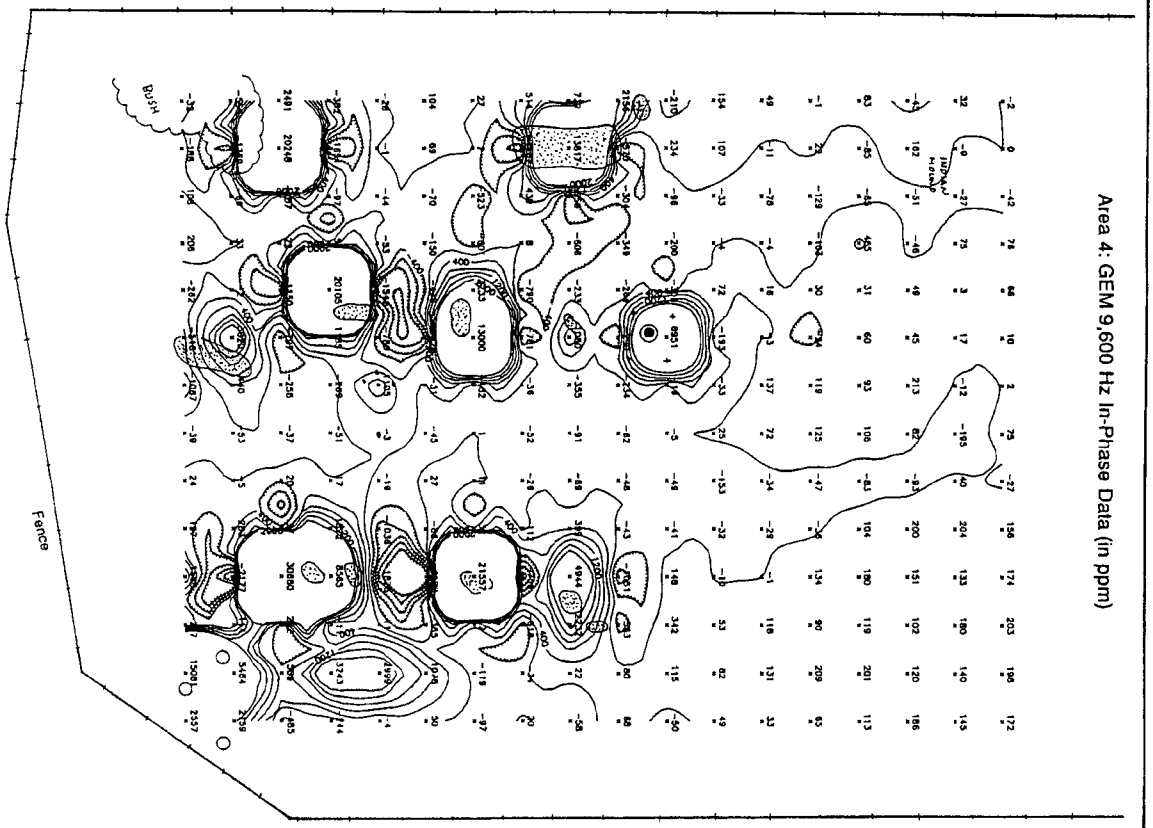

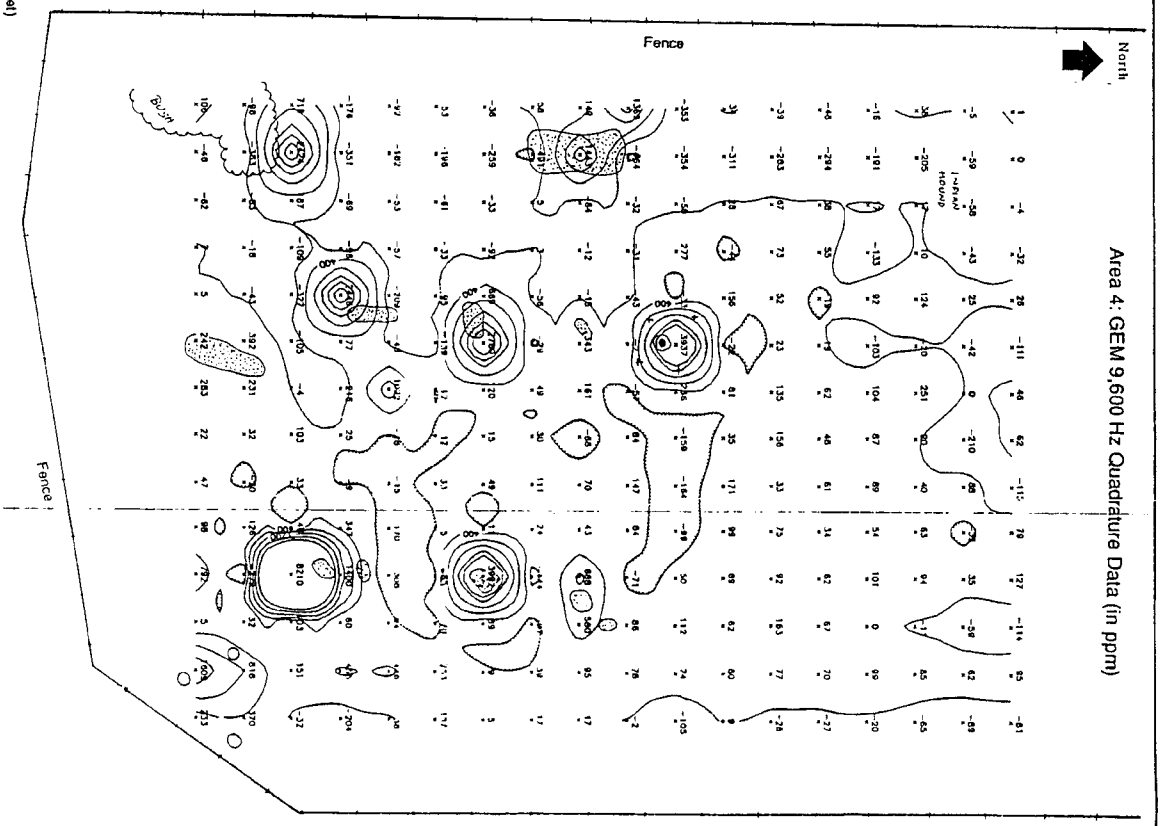

Scale (feet)
0 10 30

Geophex

Figure 3.1-6. Area 4: Electromagnetic data (in ppm); 9,600 Hz; Contour interval = 400 ppm.

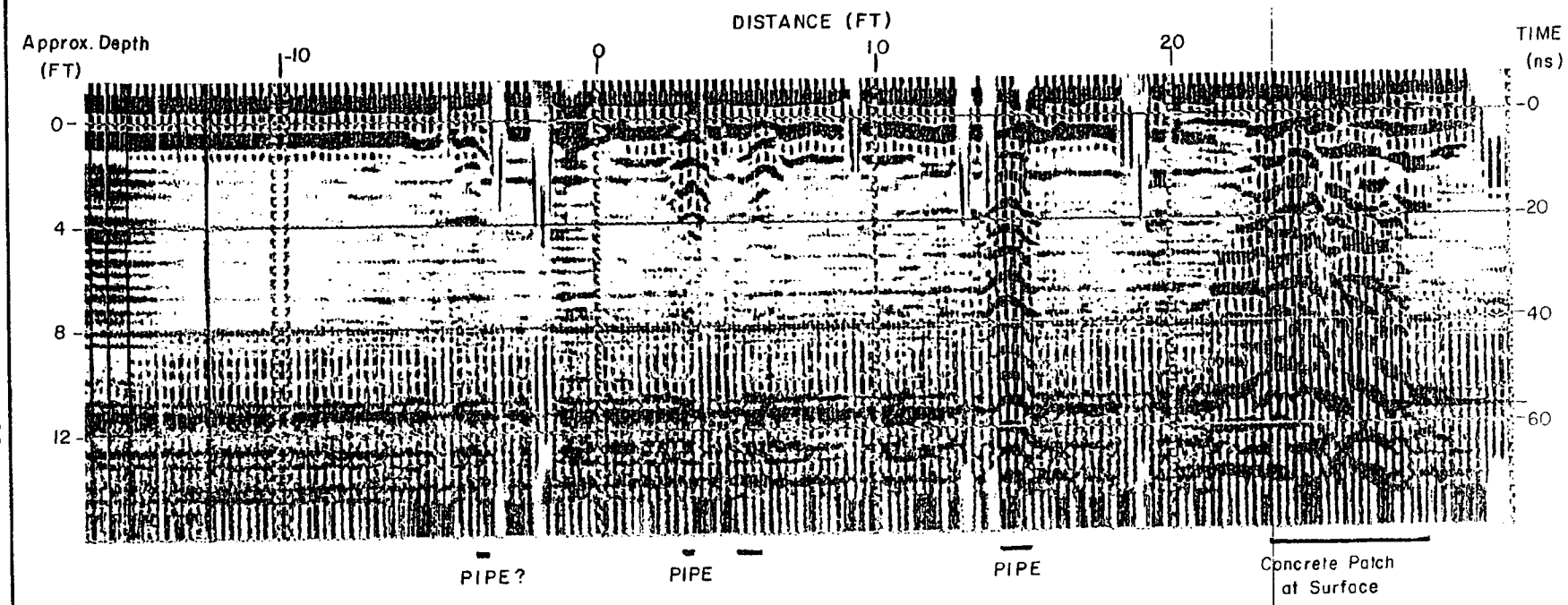

Geophex

Figure 3.1-7. Area 4: A typical GPR profile near the suspect shafts area.

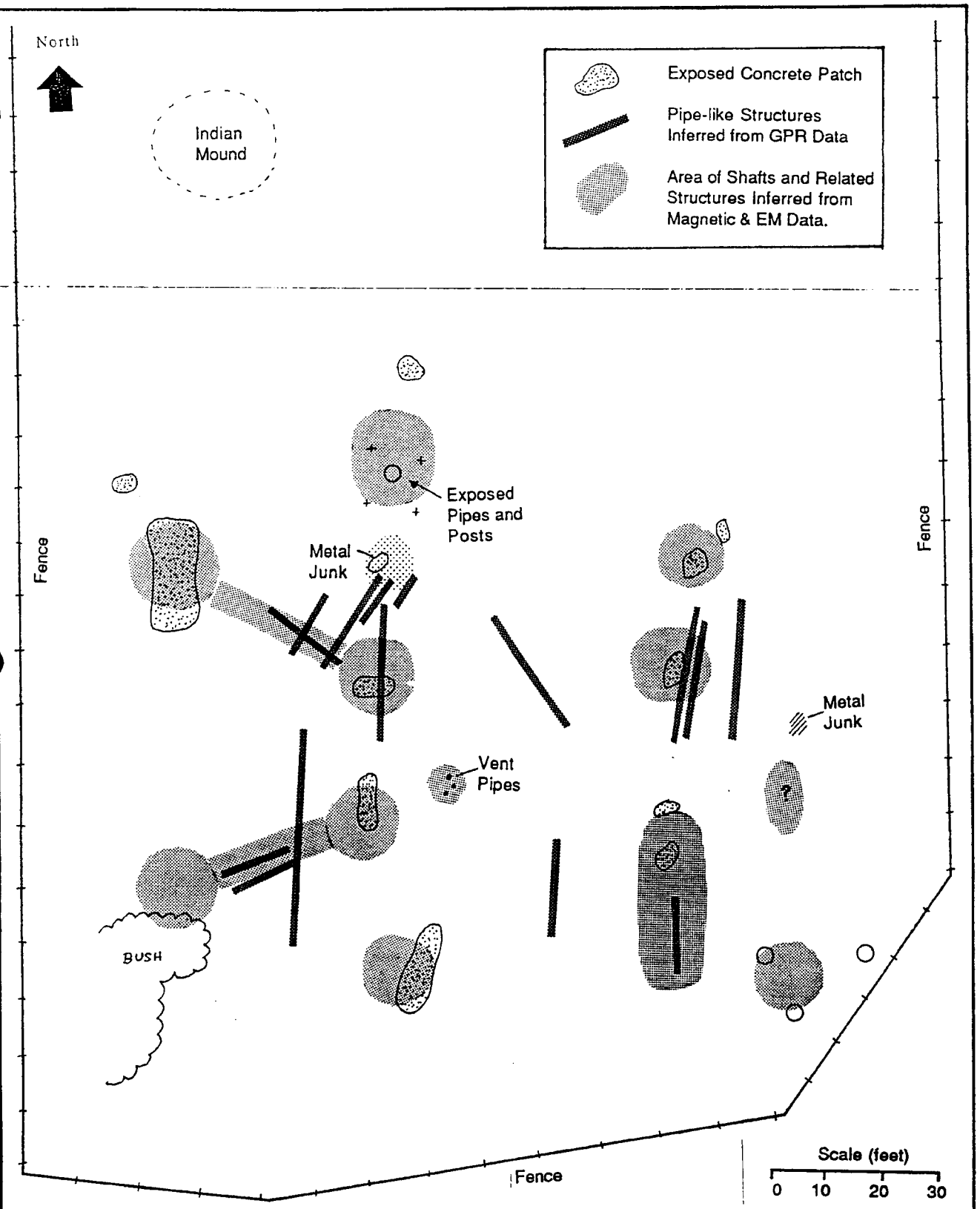

Geophex

Figure 3.1-8. Area 4 (Test Shafts): Interpretive sketch based on geophysical data and field observation.

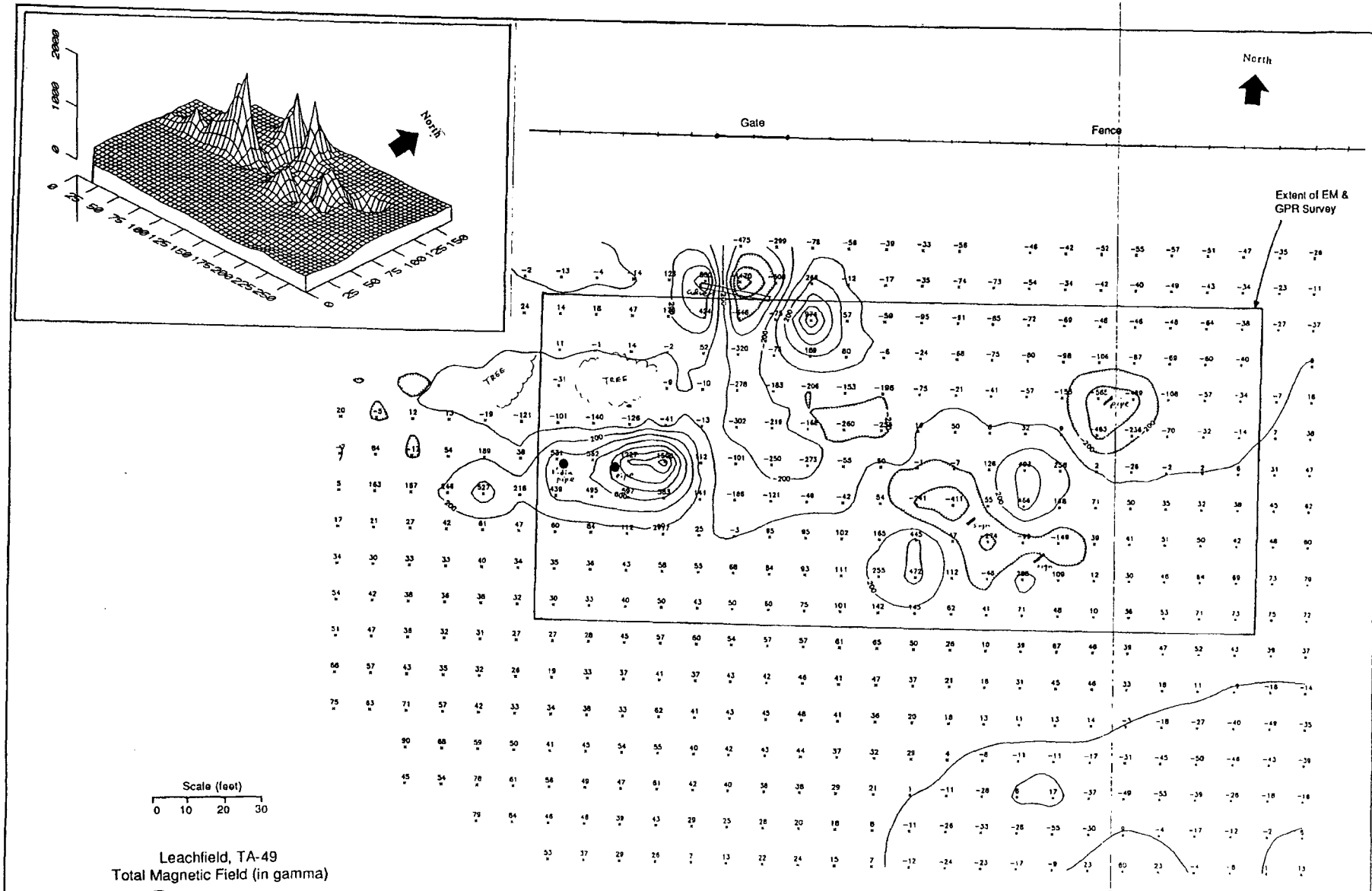

Figure 3.2-1. Area 11 (Leach Field): total field magnetic map (in gamma); Background = 52,000 gamma; Contour interval = 200 gamma.

Geophex

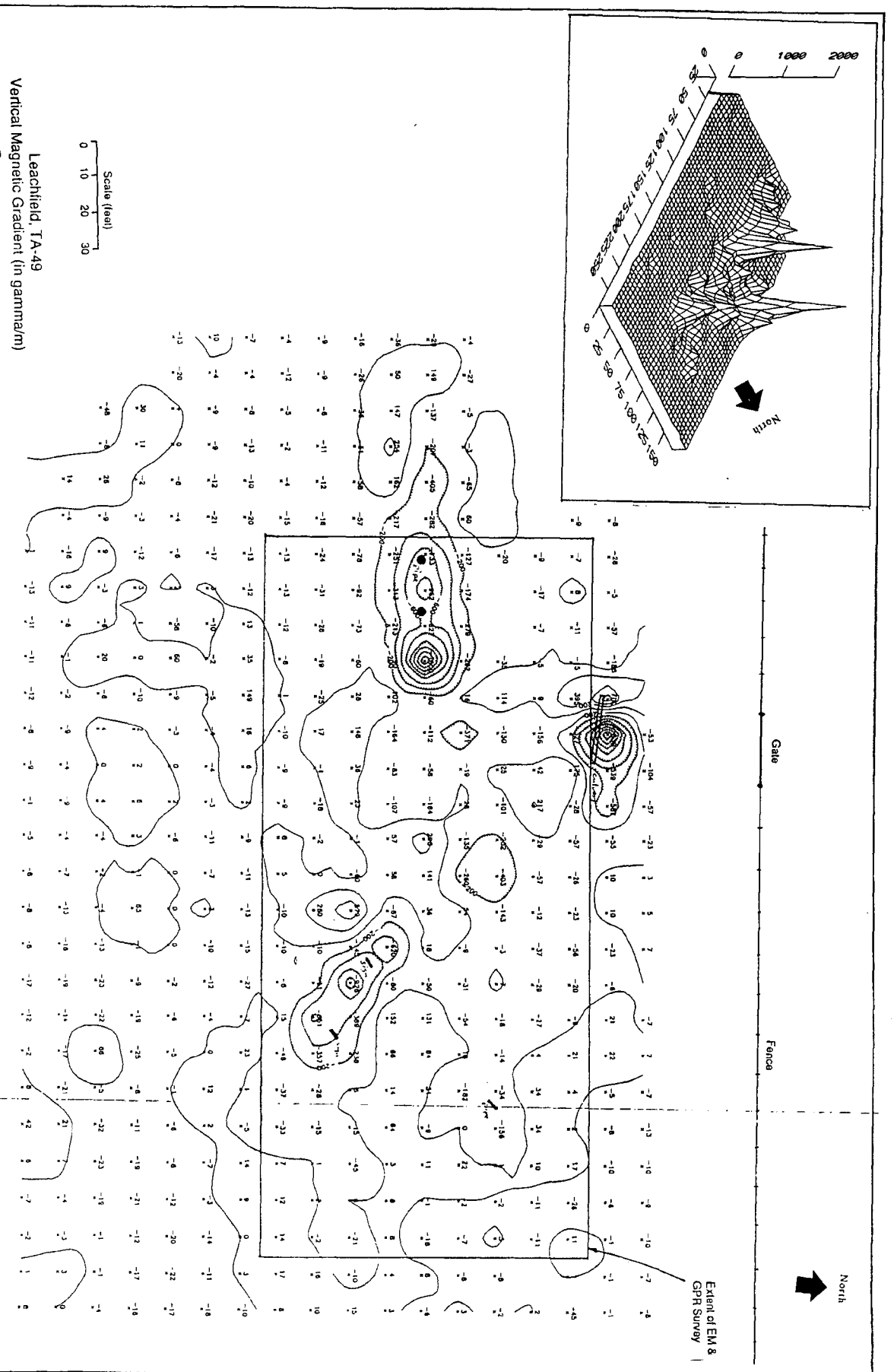

Geophex

Figure 3.2-2. Area 11: Magnetic gradient map (in gamma/m; positive-downward); Contour interval = 200 gamma/m. The fish-net view is shown upside down for a clear view.

In-Phase Data

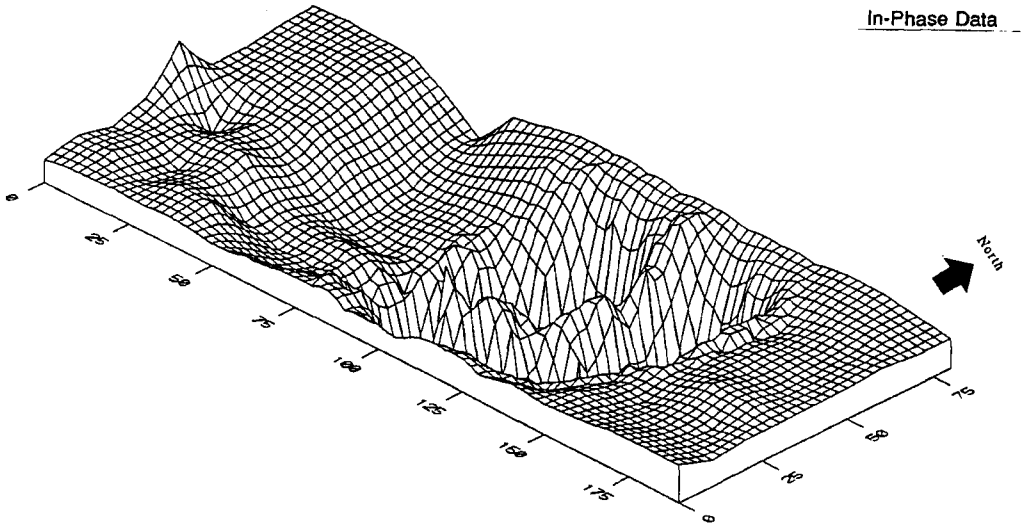

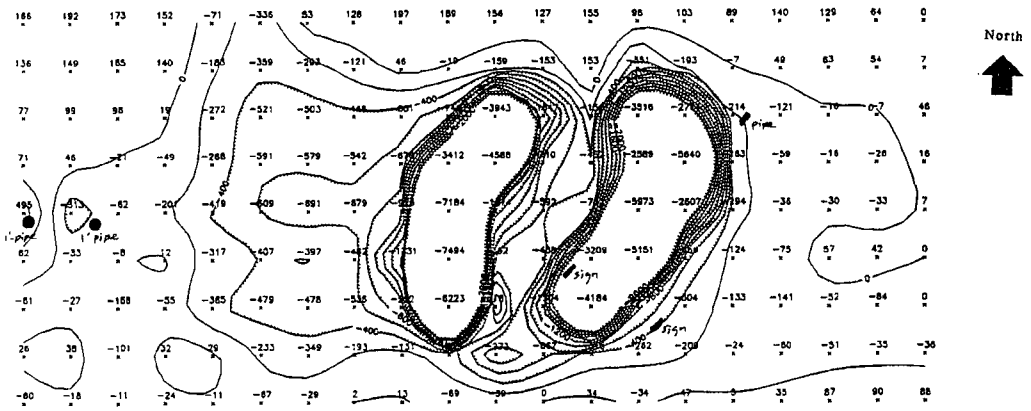

Leachfield: GEM 800 Hz In-Phase Data (in ppm)

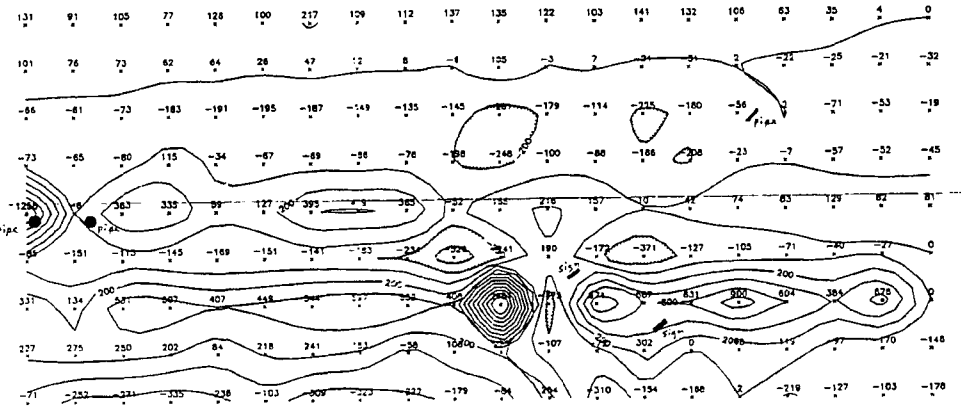

Leachfield: GEM 800 Hz Quadrature Data (in ppm)

Scale (feet)
0 10 20 30

Geophex

Figure 3.2-3. Area 11: Electromagnetic data (in ppm); 800 Hz; Contour interval = 200ppm.

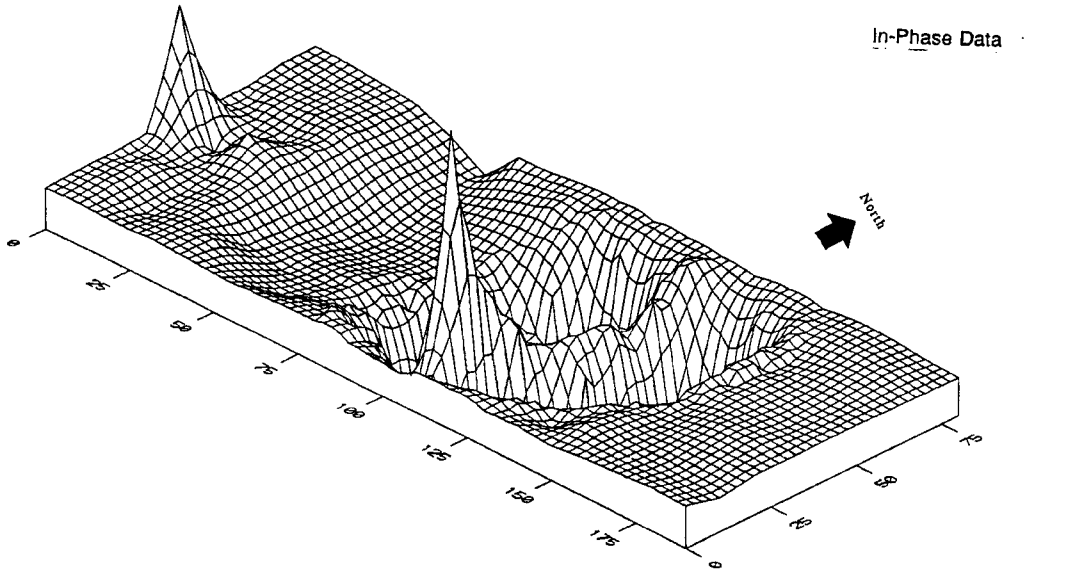

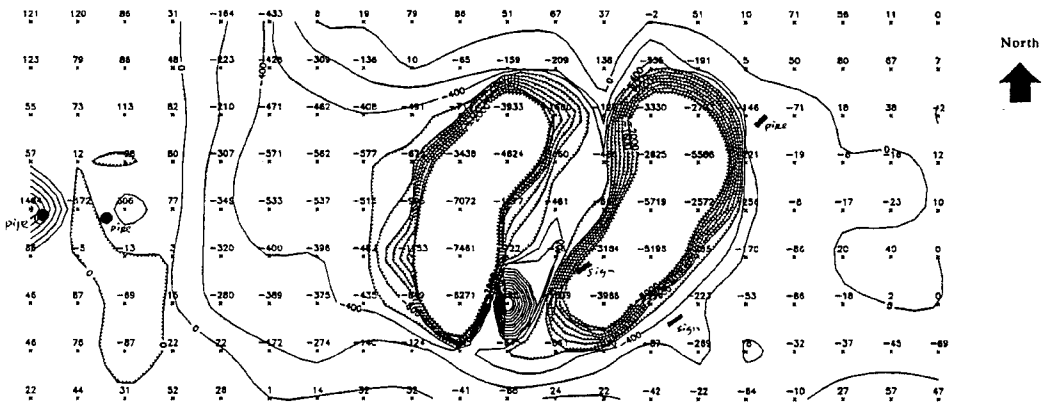

Leachfield: GEM 3,200 Hz In-Phase Data (in ppm)

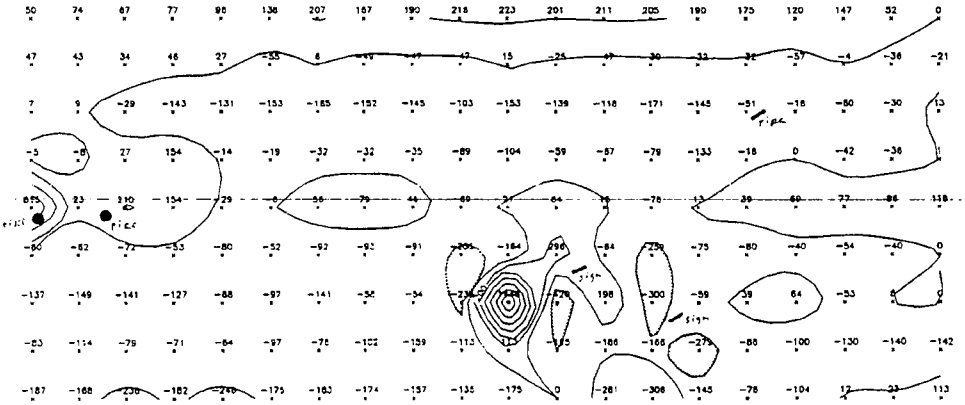

Leachfield: GEM 3,200 Hz Quadrature Data (in ppm)

Scale (feet)
0 10 20 30

Geophex

Figure 3.2-4. Area 11: Electromagnetic data (in ppm); 3,200 Hz; Contour interval = 200ppm.

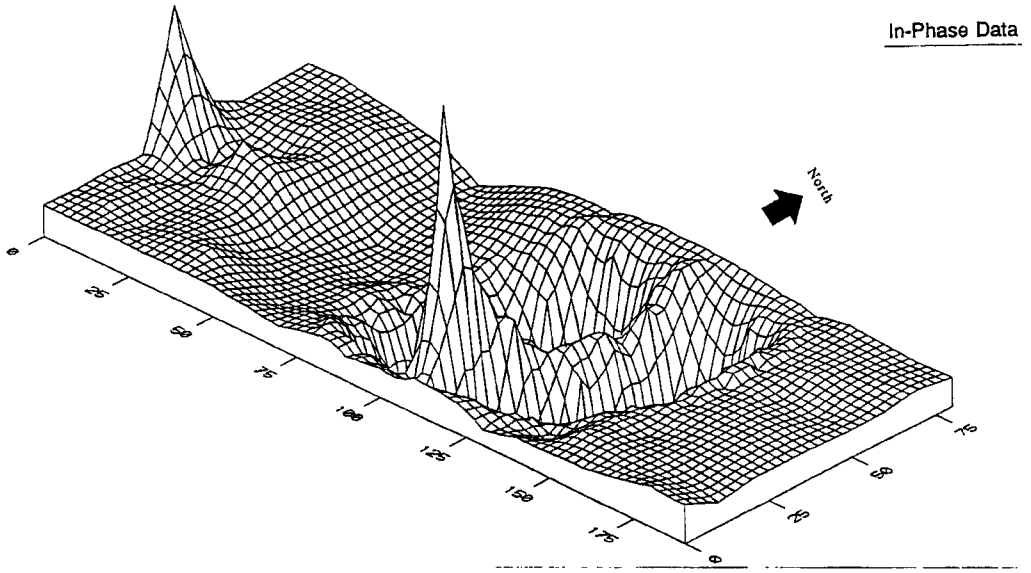

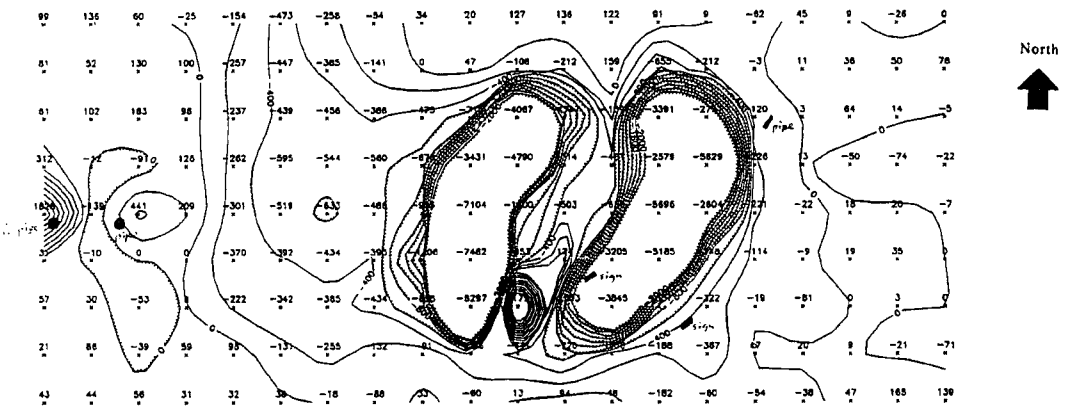

Leachfield: GEM 9,600 Hz In-Phase Data (in ppm)

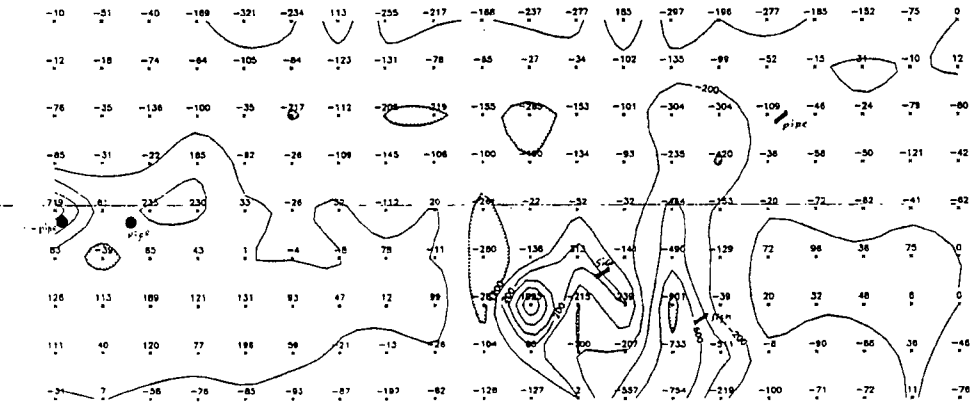

Leachfield: GEM 9,600 Hz Quadrature Data (in ppm)

Scale (feet)
0 10 20 30

Geophex

Figure 3.2-5. Area 11: Electromagnetic data (in ppm); 9,600 Hz; Contour interval = 200ppm.

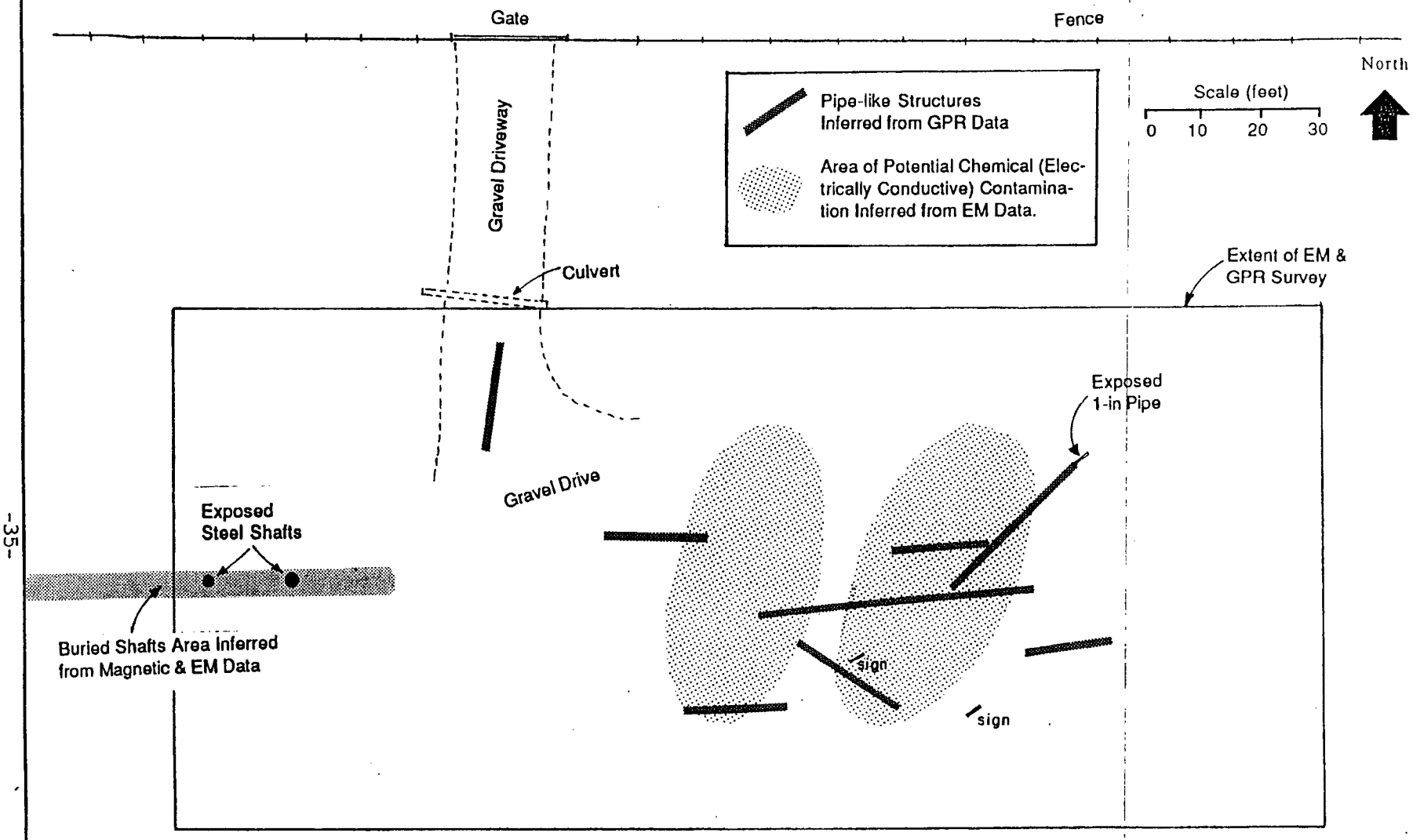

Geophex

Figure 3.2-6. Area 11 (Leach Field): Interpretive sketch based on geophysical data and field observation.

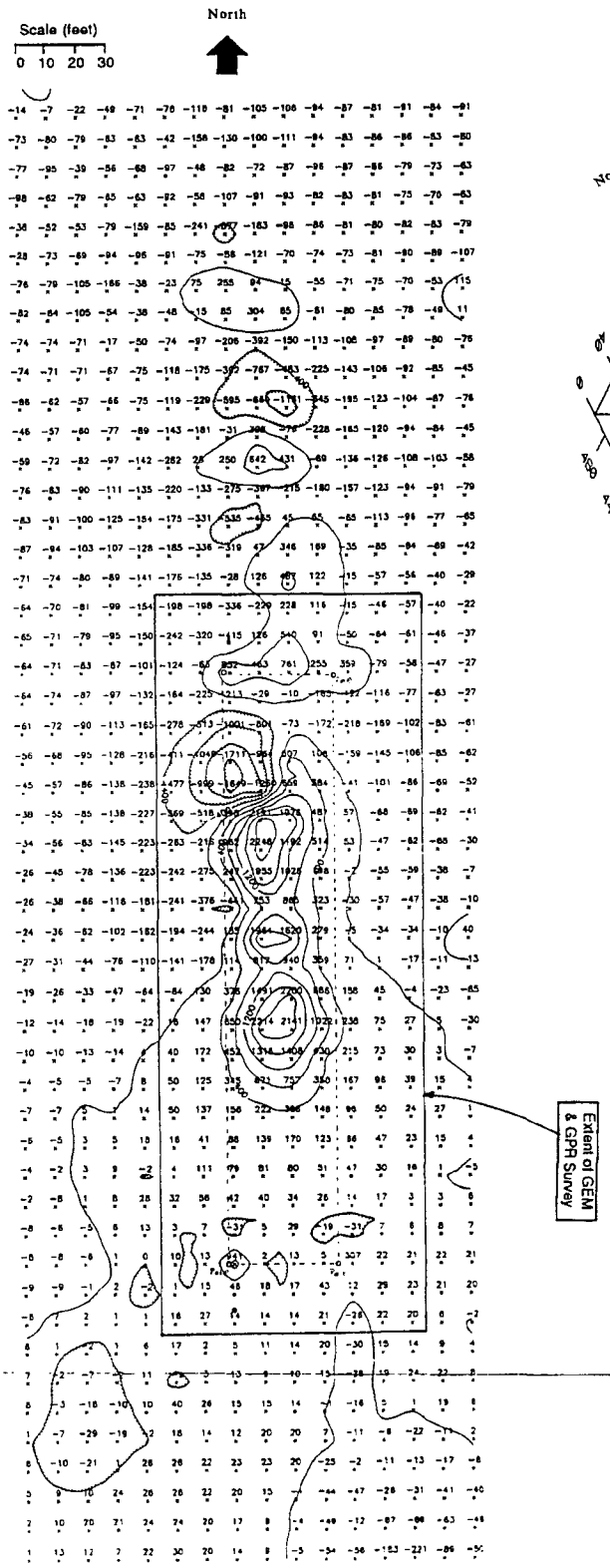

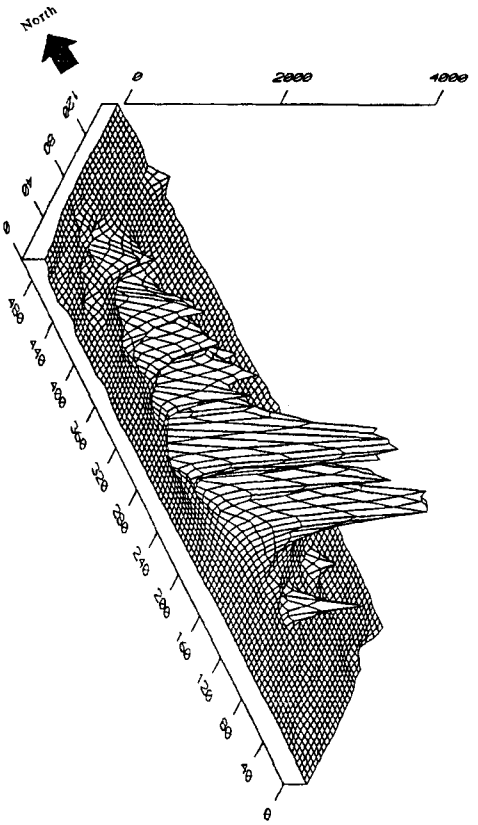

Landfill, TA-49:
Total Field Magnetic Data

Geophex

Figure 3.3-1. Landfill: Total field magnetic map (in gamma); Background = 52,200 gamma; Contour interval = 400 gamma.

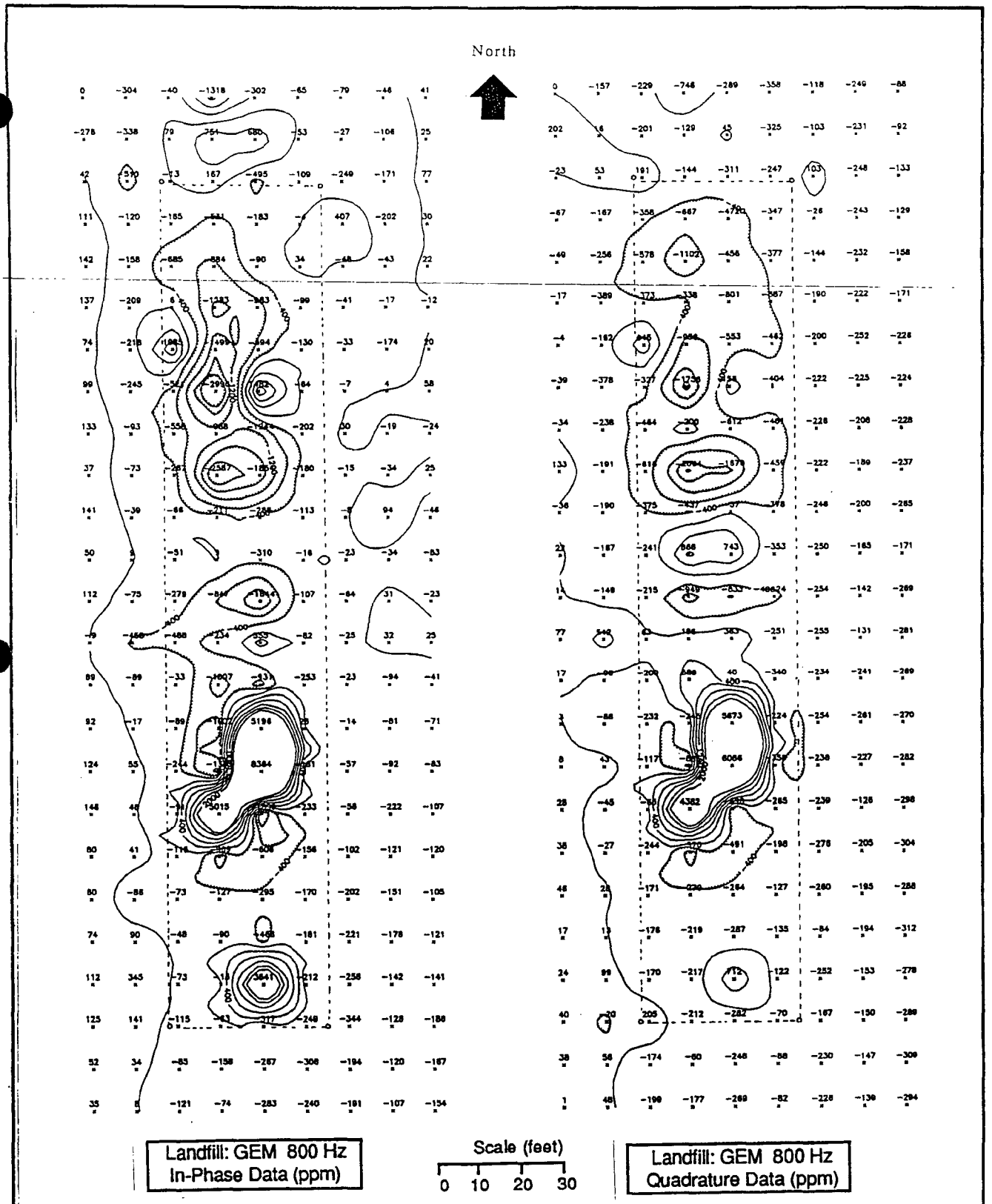

Geophex

Figure 3.3-2. Landfill: Electromagnetic data (in ppm); 800 Hz; Contour interval = 400 ppm.

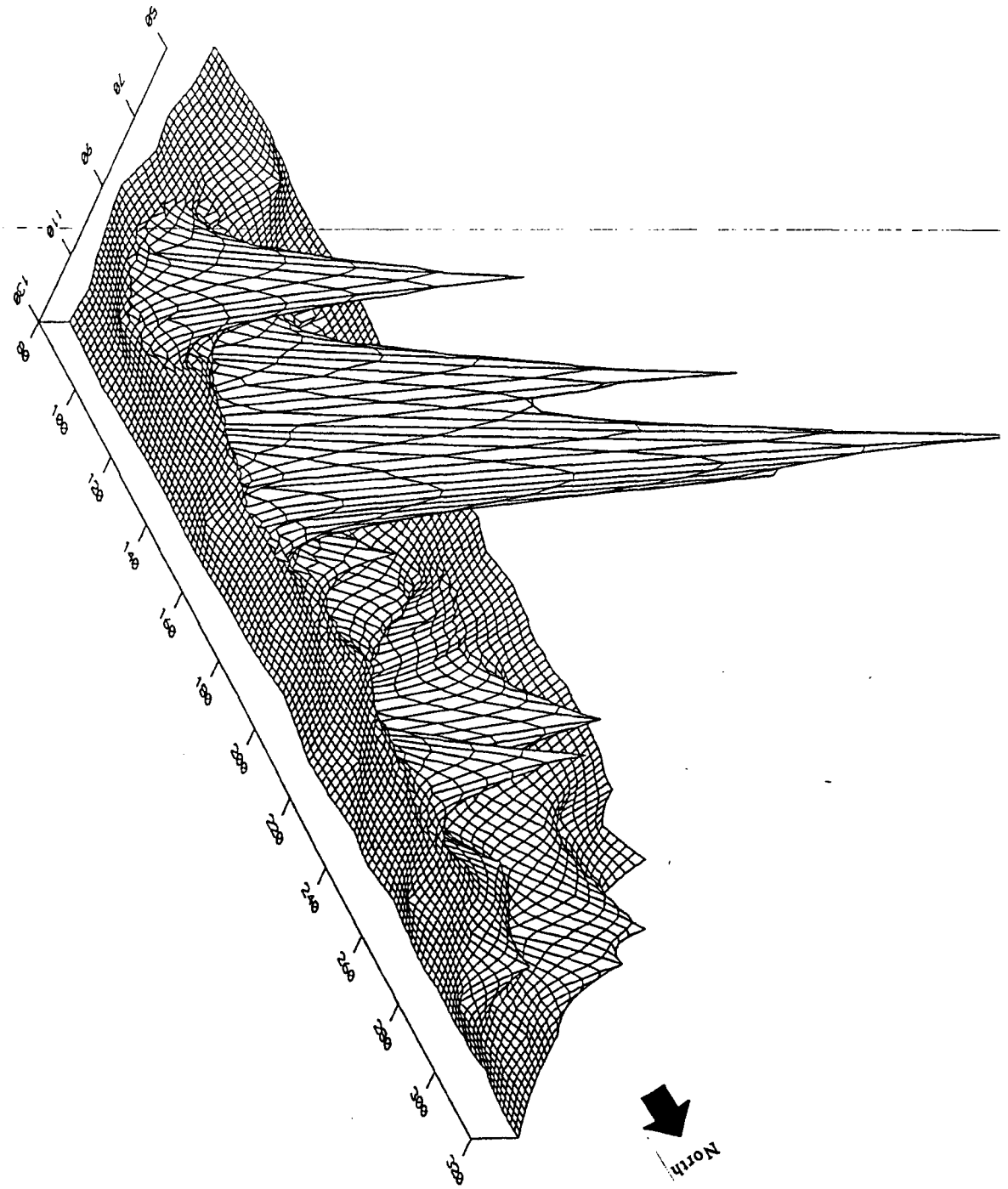

Geophex

Figure 3.3-3. Landfill: Fish-net view of electro-magnetic data (in ppm); 800 Hz Inphase data.

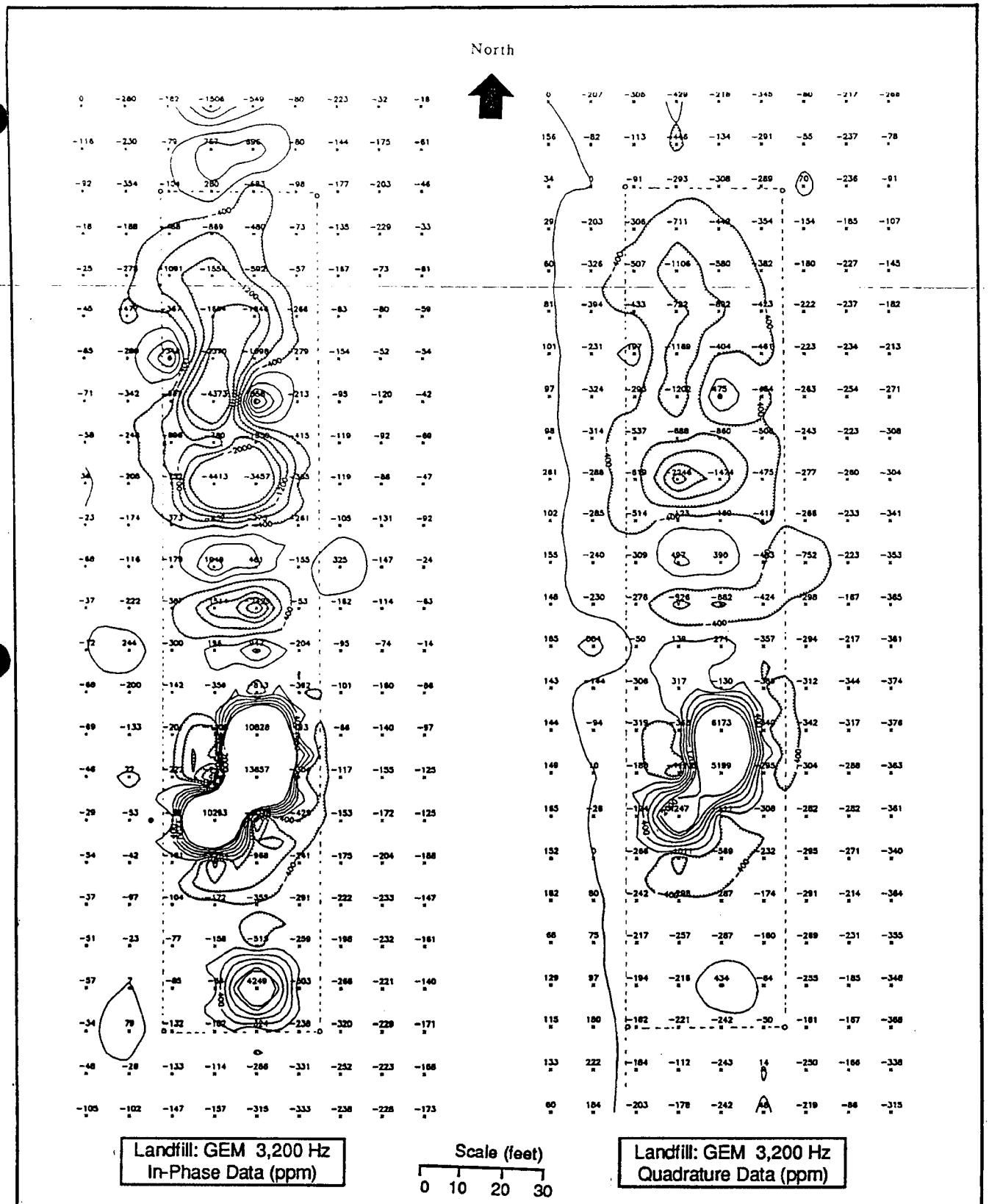

Geophex

Figure 3.3-4. Landfill: Electromagnetic data (in ppm); 3,200 Hz; Contour interval = 400 ppm.

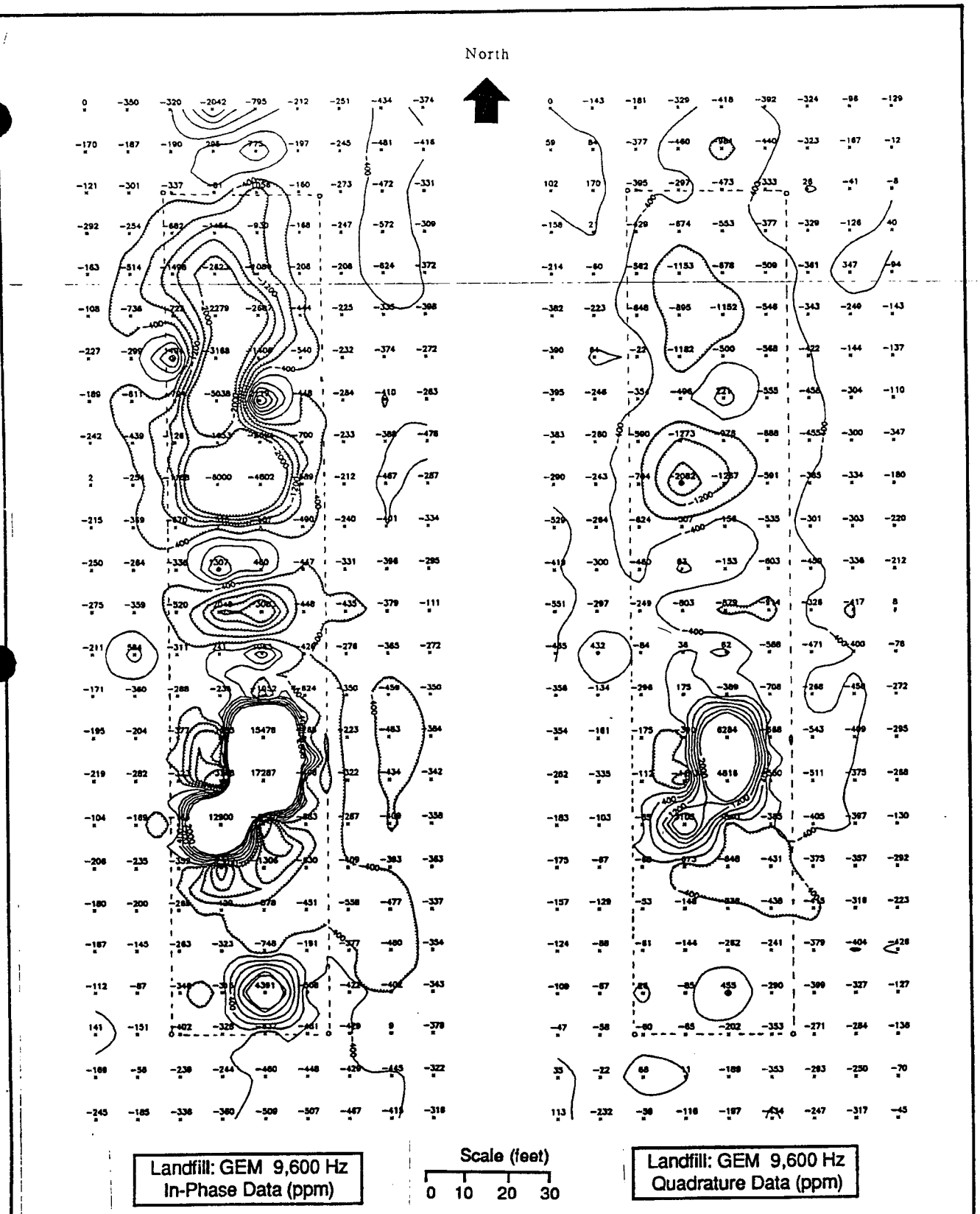

Geophex

Figure 3.3-5. Landfill: Electromagnetic data (in ppm); 9,600 Hz; Contour interval = 400 ppm.

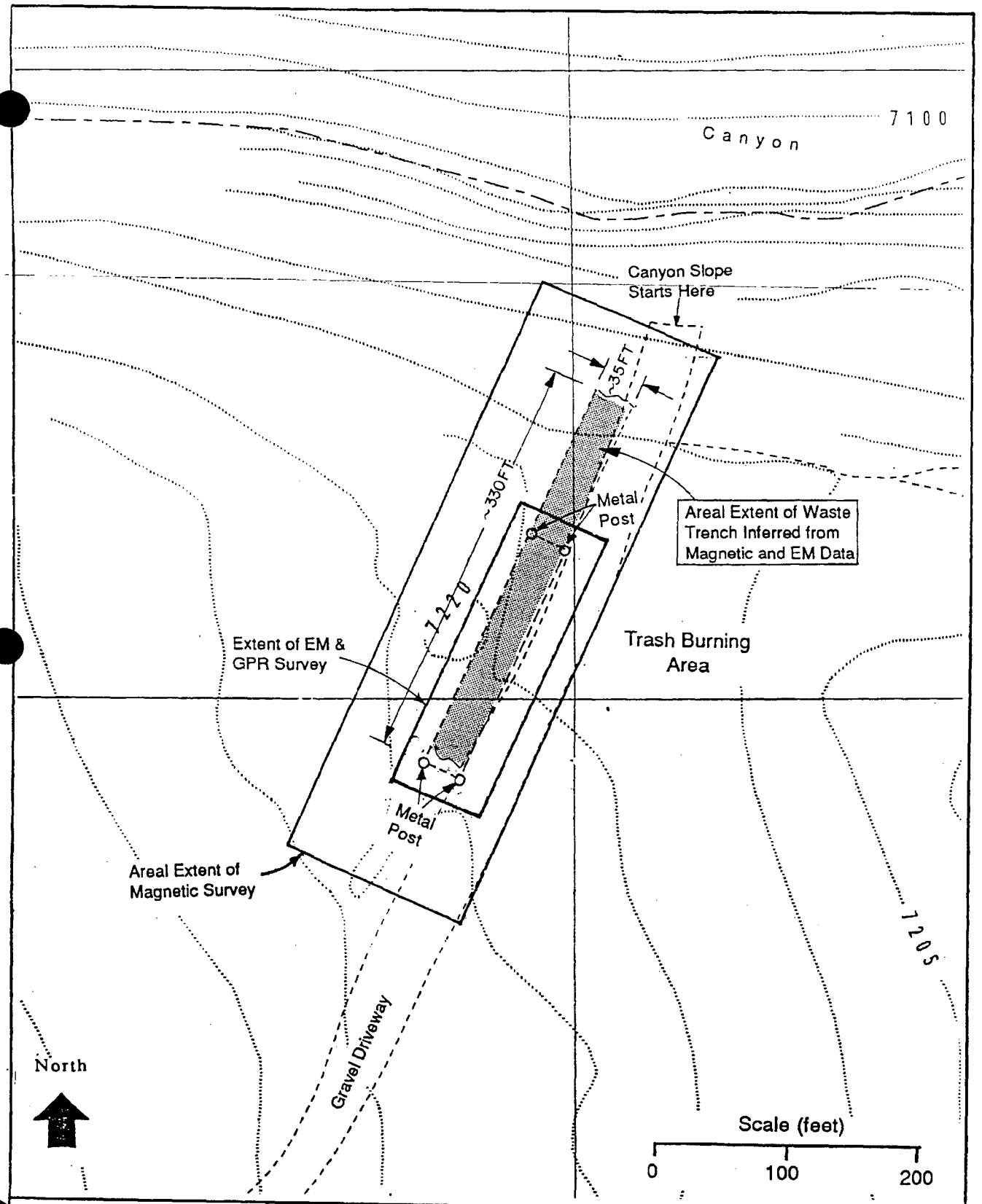

Geophex

Figure 3.3-6. Landfill: Interpretive sketch based on geophysical data and field observation.

Appendix A:

Description of Geophex Electromagnetic Sensor GEM-1

Geophex, Ltd.
605 Mercury Street
Raleigh, NC 27608-2343

Description of Geophex Electromagnetic Sensor GEM-1[1]

1. Project Summary

Geophex was awarded on September 7, 1989, by USACERL a research contract that called for development of a Portable Electromagnetic Sensor that would be able to detect metallic and nonmetallic underground storage tanks (USTs). Our original proposal, dated January 2, 1989, describes pertinent theoretical bases and proposed configuration of the hardware.

Leaking USTs (LUSTs) are one of the most pressing national environmental issues. Geophex specializes in a variety of tasks involving management and closure of USTs, as well as remedial investigations, feasibility studies, and remedial actions resulting from LUSTs. Therefore, we have our own vested interest in developing a viable instrument that can be used for locating USTs and, possibly, even mapping potential contaminant plumes and groundwater levels.

In this Phase 1 report, we describe the Geophex GEM-1 sensor that has been designed, fabricated, and tested under this contract. The laboratory test data, made over an artificial target, indicate that the PEM sensor has a typical sensitivity of about 10 parts-per-million (ppm) or 0.01 parts-per-thousand (ppt). This demonstrated sensitivity is at least an order-of-magnitude better than any existing portable electromagnetic sensors that are commercially used for finding metallic objects.

With some additional electronic improvements, a set of real-time interpretation software, and rugged packaging, GEM-1 should be exceptionally useful for environmental investigation tasks involving USTs and LUSTs. The sensor should also be useful for finding any buried objects such as utility pipes, land mines, burial trenches, and drums, as well as mapping groundwater levels, shallow geology, and possibly contaminant plumes. Based on the performance of our prototype, we recommend the scope of work under Phase 2 that would produce a production-model sensor and case histories.

2. Theoretical Basis for the PEM Sensor

The basic principle of a frequency-domain electromagnetic system involves the measurement of change in mutual impedance between a pair of coils moving over the earth. A transmitter coil sets up a sinusoidally varying primary field that induces a system of currents within the earth

1. An abbreviated version of Final Report submitted by Geophex to the US Army Construction Engineering Research Laboratory, entitled "Development of an Electromagnetic Sensor to Detect Metallic and Nonmetallic Underground Storage Tanks:USACERL Contract No. DACA88-89-C-0013, dated April, 1990.

below. This induced current, in turn, generates a secondary magnetic field that is measured by a receiver coil. The fundamental equations describing the magnetic field generated by a dipole located at or above the surface of a layered earth are known to the geophysical community and will not be presented here. Some recent literature relevant to this electromagnetic sensor development are included in the references.

When the two coils are maximum coupled (i.e., in a mutually co-planar or coaxial configuration), the primary field at the receiver coil is very strong compared to the magnitude of the secondary induced field. It is desirable to remove this large field, mainly to reduce the dynamic range needed for the receiver preamplifier circuit. This can be accomplished by using a third coil, commonly termed a "bucking coil," that is placed between the transmitter and receiver coils.

The bucking coil is made so that its induced voltage from the primary field in the absence of the earth (i.e., in free space) is equal to that induced in the receiver coil. The bucking coil and the receiver coil are wired in opposing (or bucking) polarity. By eliminating the primary field, the combined sensor unit thus produces a zero output in free space. When a conductive body (e.g., a steel UST) is present nearby, the sensor produces a differential output depending only on the geometry and conductivity structure of the body.

The secondary field detected by the sensor is split into in-phase and quadrature (out-of-phase) components, which are expressed in ppm or ppt against the primary field strength that would have been induced in an unbucked receiver coil. This complex quantity (real and imaginary) is called the mutual coupling ratio, and it becomes the basis for subsequent data interpretation.

3. General Description of GEM-1

During Phase 1, we designed, fabricated, and tested all electronic components in laboratory. Figure 1 shows the basic electronic block diagram of GEM-1 sensor as well as the packaging for sensor coils and a console. Prototype instrument dimensions are also shown in the figure.

This system is designed to minimize temporal drift and to insure calibration stability. The transmitter waveform is generated by means of a power H-bridge consisting of high-current Mosfet switching transistors. This H-bridge switches a DC voltage at a switching rate of about 76.8 kHz. The bridge, in turn, is digitally controlled by a Digital Sequence Generator (DSG) that feeds a binary series pre-recorded in a ROM (read-only memory) into a Pulse Former. The output current waveform in the transmitter, thus, is digitally constructed by the binary series by means of a well-established pulse-width modulation (PWM) technique. This binary series contains all the codes for a desired frequency constituent.

The receiver coil detects the earth response from below. The bucking coil is designed to cancel the strong primary field and also to produce the transmitter reference waveform. Both the signal and reference outputs from the receiver circuits are given to a Signal Processor unit that

consists of an analog-to-digital (A/D) converter and a high-speed digital convolver.

Since we know precisely the transmitted waveform, the convolver (essentially a multiply and accumulate function, i.e., convolution) is instructed to pick only the original transmitter frequency. This is accomplished by convolving the incoming signals with pre-programmed sine and cosine series (coinciding with the transmitter frequency) stored in a RAM (random access memory) look-up table. This detection scheme results in an extremely narrow bandwidth and, thus, enhances the signal-to-noise ratio (SNR) by an order of magnitude or more. These digitally processed data constitute the raw survey data.

Any metallic object other than the coils, such as the main console, generates a strong secondary field. This effect can be minimized by placing it at a strategic location, where the secondary field, as seen by the receiver, is at a minimum. A specific location exists between the receiver and the bucking coils. This is an original technique developed at Geophex and used successfully for an airborne EM sensor for the US Navy. The main console is, thus, located at a precisely calculated station.

In addition to the precise location, the console is packaged in an electromagnetically shielded pod. The shielding isolates any direct radiation between the various electronic circuits and the sensor coils. The main tube has a 4-inch diameter and is made of Kevlar-epoxy material. Kevlar is a light and rigid synthetic material having very favorable thermal properties for the proposed sensor.

4. Hardware Descriptions

The sensor is electronically partitioned into three sub-units, viz:

- Control Processor Unit (CPU): runs the system and reduces the raw sampled data,
- Amplifier and A/D Unit: amplifies and filters the incoming signals and converts them to a digital format, and
- Transmitter Unit: generates timing signals and drives the transmitter coil using a power H-bridge.

All three sub-units are housed in a single console (of about 4-inch by 4-inch by 8.8-inch rectangular box) located approximately at the midpoint. In this section, we present a functional description for each sub-unit.

4.1 Control Processor Unit (CPU)

The CPU contains a microprocessor that collects and processes the PEM data. The heart of the control processor is the Motorola 56001 CPU chip. One of its major features is an arithmetic unit containing a 24-bit parallel multiplier and two 56-bit accumulators. The advantage of this architecture is the ability to perform high-precision multiplications with little

chance of overflow.

The other two parts of the control processor are the memory and the input/output (I/O) system. The memory used is a combination of low-power EPROM (erasable programmable read-only memory) and low-power static RAM. The EPROM is configured as a 64K-word, one-word containing 24 bits. The RAM has a battery-backup for power-off data retention and is organized into two banks of 64K-words. The memory is decoded using a programmable logic device so that, during development, segments of RAM may be used for program verification.

The I/O system is composed of various general-purpose I/O lines available from the CPU, one Read-Write port used for reading and writing to the console, and one serial port used for transferring data and programs from the computer host. The host port on the 56001 is used as a general purpose port for controlling various functions of the receiver and transmitter and for monitoring the system status. The Read-Write Port is used for writing to the LCD display and for reading the positions of the panel buttons and the dip switch. The serial port is connected directly to an RS-232 driver chip.

One feature of the system is its ability to go into a standby mode that draws very little power. The 56001 has a STOP instruction which stops both the processor and the clock generator. When stopped, the current draw of the digital section is about 5 mA, a significant advantage for a battery powered instrument. Pressing any one of the panel buttons will trigger an INTERRUPT which will restart the processor.

4.2 Amplifier and A/D Converter Unit

This unit is designed as a dual-channel, differential amplifier with level detection and gain selection on the receiver coil channel. The two amplifiers incorporate passive band-pass filters having very high stability in their frequency response. The A/D converter has built-in digital low-pass filters with very sharp roll-off. These anti-aliasing filters eliminate the need for over-sampling. The signal channel amplifier has an input-referenced noise of less than $1nV/\sqrt{Hz}$ over the sampled band-width and has a common-mode noise rejection (CMNR) ratio greater than 115 dB.

4.3 Transmitter Unit

This unit consists of a clock divider, an EPROM addressed with a counter, and a monolithic power H-bridge. The clock divider is made using two ripple counters and a programmable logic device. This divider provides the timing signals needed for both the transmitter and the A/D on the amplifier. The EPROM is pre-programmed with waveforms for all the broadcast frequencies that can be selected using one of the four address lines.

The waveforms are clocked out to the H-bridge through another programmable logic device (PLD) that provides necessary interface logic. The H-bridge, with built-in temperature and

current sensors, is a highly integrated device that provides circuitry to drive the internal FETs (field effect transistors) at an RMS (root-mean squares) current of about 3 Amperes. The bridge directly drives the transmitter coil that radiates the programmed waveforms.

Under this contract, a prototype of each sub-unit has been designed, fabricated, assembled, and tested. Real-time convolution and system control codes have been written, tested, and installed.

8. References

I.J. Won, 1983, A sweep-frequency electromagnetic exploration method, Chapter 2, in *Development of Geophysical Exploration Methods-4*, Editor; A.A. Fitch, Elsevier Applied Science Publishers, Ltd., London, pp. 39-64.

I.J. Won, 1985, Frequency-domain electromagnetic ice-sounding, in *Proceeding of the Arctic Oceanography Conference*, NSTL, Mississippi, pp. 167-172.

I.J. Won, 1986, High-resolution electromagnetic altimetry over the ocean, *IEEE Journal of Ocean Engineering*, Vol. OE-11, pp. 327-332.

I.J. Won and K. Smits, 1986, Application of the airborne electromagnetic method for the bathymetric charting in shallow oceans, in *Proceedings of Airborne Resistivity Workshop*, Canada Geological Survey, Paper 86-22, pp. 99-106, Ottawa.

I.J. Won and K. Smits, 1987, Airborne electromagnetic measurements of electrical conductivities of seawater and bottom sediments over shallow ocean, *Marine Geotechnology*, Vol. 7, pp. 1-14.

I.J. Won and K. Smits, 1990, Airborne Electromagnetic Bathymetry, in *Developments and Applications of Modern Airborne Electromagnetic Surveys*, Edited by D.V. Fitterman, US Geological Survey Bulletin 1925, pp. 155-164.

I.J. Won and K. Smits, 1991, Airborne Electromagnetic Bathymetry, *Geoexploration*, Special Issue: Development in Geophysical Exploration Methods, Edited by A.A. Fitch, Vol. 27, pp. 297-319.

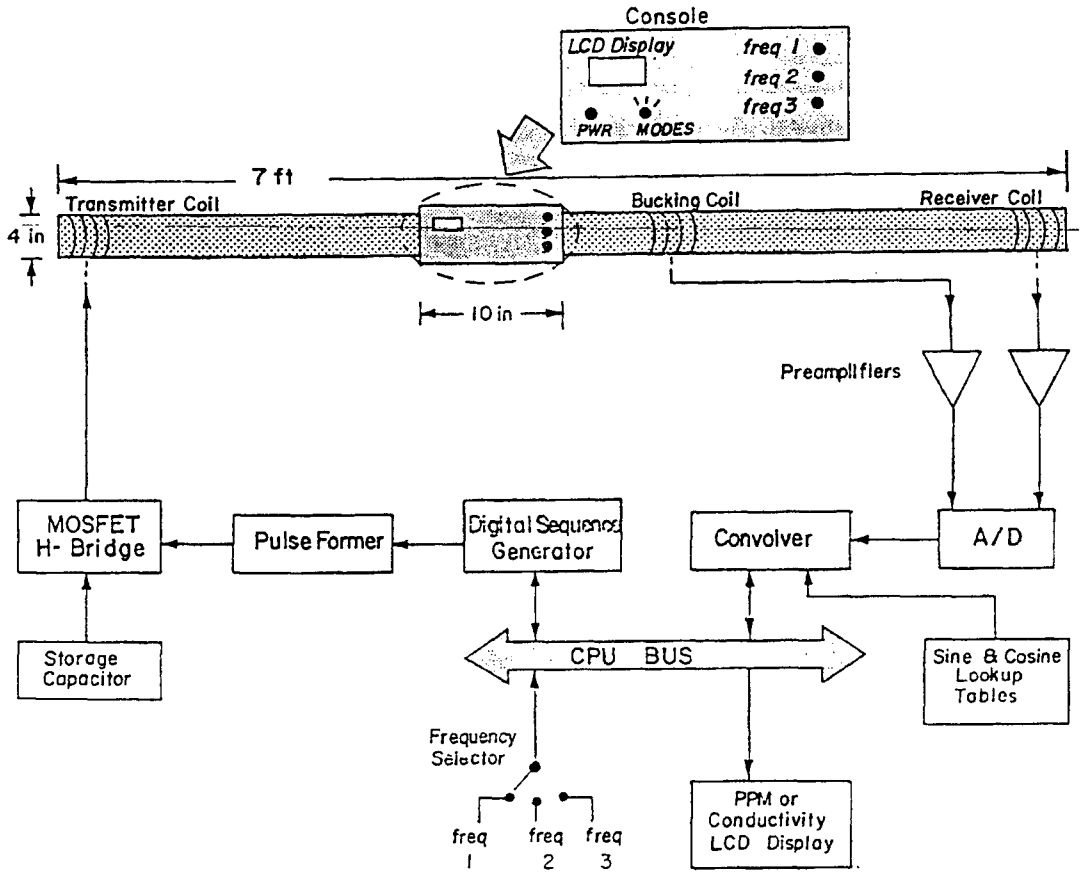

Figure 1. Electronic block diagram and a possible packaging of the proposed portable EM sensor.

ERID#: 8887	LOS ALAMOS NATIONAL LABORATORY ENVIRONMENTAL RESTORATION (RRES-R) Records Processing Facility ER Records Index Form

Date Received: 8/27/1992 ***Processor:*** GAA ***Page Count:*** 52

Privileged: (Y/N) N ***Record Category:*** R ***Administrative Record: (Y/N)*** Y

FileFolder: N/A

Miscellaneous Comments: CONTRACT NO. 9-L61-W0086-1

Record Documents:

Start Pg	Doc Type	Doc Date	Title	Box	Package
1	REPORT	8/1/1991	FINAL REPORT ON A PILOT STUDY ON THE APPLICABILITY OF SELECTED GEOPHYSICAL METHODS TO THE INVESTIGATION OF THREE ENVIRONMENTAL SITES IN TA-49, LOS ALAMOS NATIONAL LABORATORY	20	